การพัฒนาไมโครนีเดิลส์ที่บรรจุกรดแกมมา-แอมิโนบิวไทริกเพื่อนำส่งทางผิวหนัง

นายกฤชพล ปานรอด

วิทยานิพนธ์นี้เป็นส่วนหนึ่งของการศึกษาตามหลักสูตรปริญญาวิทยาศาสตรมหาบัณฑิต
สาขาวิชาวิทยาศาสตร์เครื่องสำอาง ภาควิชาวิทยาการเภสัชกรรมและเภสัชอุตสาหกรรม
คณะเภสัชศาสตร์ จุฬาลงกรณ์มหาวิทยาลัย
ปีการศึกษา 2559

DEVELOPMENT OF MICRONEEDLES CONTAINING *GAMMA*-AMINOBUTYRIC ACID FOR SKIN DELIVERY

Mr. Kritchapol Panrod

A Thesis Submitted in Partial Fulfillment of the Requirements
for the Degree of Master of Science Program in Cosmetic Science
Department of Pharmaceutics and Industrial Pharmacy
Faculty of Pharmaceutical Sciences
Chulalongkorn University
Academic Year 2016

Thesis Title	DEVELOPMENT OF MICRONEEDLES CONTAINING *GAMMA*-AMINOBUTYRIC ACID FOR SKIN DELIVERY
By	Mr. Kritchapol Panrod
Field of Study	Cosmetic Science
Thesis Advisor	Assistant Professor Vipaporn Panapisal, Ph.D.
Thesis Co-Advisor	Anyarporn Tansirikongkol, Ph.D.
	Assistant Professor Werayut Srituravanich, Ph.D.

Accepted by the Faculty of Pharmaceutical Sciences, Chulalongkorn University in Partial Fulfillment of the Requirements for the Master's Degree

.....Dean of the Faculty of Pharmaceutical Sciences
(Assistant Professor Rungpetch Sakulbumrungsil, Ph.D.)

THESIS COMMITTEE

.....Chairman
(Associate Professor Pornpen Werawatganone, Ph.D.)
.....Thesis Advisor
(Assistant Professor Vipaporn Panapisal, Ph.D.)
.....Thesis Co-Advisor
(Anyarporn Tansirikongkol, Ph.D.)
.....Thesis Co-Advisor
(Assistant Professor Werayut Srituravanich, Ph.D.)
.....Examiner
(Jutarat Kitsongsermthon, Ph.D.)
.....External Examiner
(Associate Professor Ubonthip Nimmannit, Ph.D.)

กฤชพล ปานรอด : การพัฒนาไมโครนีเดิลส์ที่บรรจุกรดแกมมา-แอมิโนบิวไทริกเพื่อนำส่งทางผิวหนัง (DEVELOPMENT OF MICRONEEDLES CONTAINING *GAMMA*-AMINOBUTYRIC ACID FOR SKIN DELIVERY) อ.ที่ปรึกษาวิทยานิพนธ์หลัก: ผศ. ภญ. ดร. วิภาพร พนาพิศาล, อ.ที่ปรึกษาวิทยานิพนธ์ร่วม: อ. ภญ. ดร.อัญญพร ตันศิริคงคล, ผศ. ดร.วีระยุทธ ศรีธุระวานิช, หน้า.

แกมมา-แอมิโนบิวไทริกแอซิด (กาบา) ถูกรายงานว่ามีประโยชน์ต่อผิว เนื่องจากกาบาเป็นสารขนาดโมเลกุลเล็กและละลายน้ำได้ ทำให้มีปัญหาในการผ่านชั้นผิวหนังกำพร้าไปยังบริเวณที่ออกฤทธิ์ ดังนั้นการสร้างไมโครนีเดิลส์รูปแบบใหม่ด้วยพลาสติกชนิดโพลีโพรไพลีนถูกสร้างขึ้นเพื่อที่จะเป็นตัวนำส่งกาบา การสร้างไมโครนีเดิลส์รูปแบบใหม่และกาบาที่ถูกบรรจุในไมโครนีเดิลส์ที่มีความสูง 1 มิลลิเมตรและขนาดความลึกของหลุมต่างกันสองขนาด (1 มิลลิเมตรและ 1.5 มิลลิเมตร) ถูกประเมินคุณสมบัติทั้งในด้านกายภาพและด้านเคมี ไมโครนีเดิลส์ชนิดโพลีโพรไพลีนถูกเตรียมขึ้นสำเร็จ ทำการศึกษาและประเมินคุณสมบัติทางกายภาพ ได้แก่ ลักษณะทางกายภาพของไมโครนีเดิลส์ ความแข็งแรงของไมโครนีเดิลส์ต่อแรงกดในแนวตรง และการเจาะทะลุผิวหนัง พบว่าไมโครนีเดิลส์ทั้งสองขนาดที่ถูกสร้างขึ้นมีความสูงเฉลี่ยเท่ากับ 1.03 ± 0.15 และ 1.01 ± 0.15 มิลลิเมตร ตามลำดับ ซึ่งพบว่าไม่แตกต่างกันอย่างมีนัยสำคัญ แต่มีความลึกเฉลี่ยของหลุมบรรจุยาแตกต่างกันอย่างมีนัยสำคัญ คือ 0.96 ± 0.09 และ 1.46 ± 0.09 มิลลิเมตร ตามลำดับ ไมโครนีเดิลส์ทั้งสองชนิดสามารถทนต่อแรงกดทับ (6 นิวตัน/เข็มต่อแรงกดแนวตรง) ปราศจากการแตกหักหรือเสียรูปอย่างมีนัยสำคัญจากการทดสอบความแข็งแรง สำหรับคุณสมบัติทางเคมี ไมโครนีเดิลส์ทั้งสองชนิดที่ถูกสร้างจากระยะความลึกของหลุม 1 มิลลิเมตร และ 1.5 มิลลิเมตร สามารถบรรจุกาบาในปริมาณที่แตกต่างกันอย่างมีนัยสำคัญ คือ 551.25 และ 715.25 ไมโครกรัมต่อแผ่น ตามลำดับ ซึ่งสัมพันธ์ไปกับขนาดของหลุมบรรจุยา กล่าวคือหลุมบรรจุยาที่มีขนาดใหญ่กว่าย่อมสามารถบรรจุกาบาได้มากกว่าที่มีขนาดเล็กกว่า ไมโครนีเดิลส์ที่ถูกพัฒนาขึ้นในการศึกษาเบื้องต้นนี้มีรัศมีปลายเข็มกว้างอย่างเป็นที่สังเกตุได้เมื่อเทียบกับไมโครนีเดิลส์ประเภทปกติ (รัศมีปลายเข็ม 252.22 ± 13.79 ไมครอนส์ สำหรับความลึกของหลุมบรรจุยา 1 มิลลิเมตร และ 233.51 ± 9.45 สำหรับความลึกของหลุมบรรจุยา 1.5 มิลลิเมตร) ด้วยเหตุดังกล่าวไมโครนีเดิลส์ทั้งสองชนิดไม่สามารถเจาะทะลุผ่านผิวหนัง แม้ว่าจะใช้แรงกดทับถึง 7 กิโลกรัม/แผ่น การพัฒนาพลาสติกไมโครนีเดิลส์ต้นแบบนี้ยังมีความจำเป็นเพื่อให้สามารถเจาะทะลุผิวหนังได้ แต่อย่างไรก็ตามจากผลการศึกษาเบื้องต้นนี้ แสดงให้เห็นว่าไมโครนีเดิลส์ต้นแบบนี้สามารถพัฒนาต่อไป เพื่อใช้เป็นระบบนำส่งสำหรับสารที่มีขนาดโมเลกุลเล็กและละลายน้ำผ่านผิวได้อย่างมีประสิทธิภาพ

ภาควิชา วิทยาการเภสัชกรรมและเภสัชอุตสาหกรรม ลายมือชื่อนิสิต .....

สาขาวิชา วิทยาศาสตร์เครื่องสำอาง ลายมือชื่อ อ.ที่ปรึกษาหลัก .....

ปีการศึกษา 2559 ลายมือชื่อ อ.ที่ปรึกษาร่วม .....

ลายมือชื่อ อ.ที่ปรึกษาร่วม .....

5676235733 : MAJOR COSMETIC SCIENCE

KEYWORDS: GABA / MICRONEEDLES / HPLC / POLYPROPYLENE / DRUG POCKET

KRITCHAPOL PANROD: DEVELOPMENT OF MICRONEEDLES CONTAINING *GAMMA*-AMINOBUTYRIC ACID FOR SKIN DELIVERY. ADVISOR: ASST. PROF. VIPAPORN PANAPISAL, Ph.D., CO-ADVISOR: ANYARPORN TANSIRIKONGKOL, Ph.D., ASST. PROF. WERAYUT SRITURAVANICH, Ph.D., pp.

Gamma-aminobutyric acid (GABA) has been reported to have several skin benefits. Since GABA is a small water soluble molecule which may have problems getting through stratum corneum to its site of action. Therefore, newly invented microneedles (MNs) fabrication of polypropylene (PP) plastic was investigated as a delivery system for GABA. Physical and chemical properties of fabricated MNs and GABA loaded MNs with height 1 mm and two different dipping distances (i.e., 1 mm and 1.5 mm) were studied. PP MNs were successfully produced. Physical properties including MNs physical appearance, the strength of MNs against axial force and skin penetration were studied. Both MNs made from different dipping distances showed no significant difference in needle height with means of 1.03 ± 0.15 and 1.01 ± 0.15 mm, respectively but showed significant difference in drug pocket depth with means of 0.96 ± 0.09 and 1.46 ± 0.09 mm, respectively. These MNs could withstand applied force (6 N/needle against axial force) without significant deformation or fracture in the failure strength tests. About the chemical property, different GABA loadings were found with MNs made from 1 and 1.5 mm dipping distances which were 551.25 and 715.25 µg GABA/piece, respectively. Loading capacities were correlated with the drug pocket size where larger pocket size could load more GABA than smaller one. These primitive fabricated MNs has noticeably wider tip radiuses (i.e., 252.22 ± 13.79 µm for 1 mm dipping distance and 233.51 ± 9.45 µm for 1.5 mm dipping distance). As a result, two produced MNs did not penetrate through the pig skin even using pressing force of 7 kg/piece. Further development of this primitive prototype of PP MNs is needed to be able to break into the skin. However, promising early results showed that the developed MNs can be a potential delivery system of small and water soluble molecule through the skin.

Department:	Pharmaceutics and Industrial Pharmacy	Student's Signature	.....
		Advisor's Signature	.....
Field of Study:	Cosmetic Science	Co-Advisor's Signature	.....
Academic Year:	2016	Co-Advisor's Signature	.....

ACKNOWLEDGEMENTS

Measureless appreciation and thankful gratitude are extended to the significant efforts of many people who help and/or give valuable knowledge, precious time and financial support in this long way of journey.

This thesis would not have been possible unless the persistent help from my thesis advisor, Assistance Professor Vipaporn Panapisal, Ph.D. with co-advisors, Anyarporn Tansirikongkol, Ph.D. and Assistance Professor Werayut Srituravanich, Ph.D. I would like to express my profound thank-you for their valuable guidance, financial support and incredible patience during the entire research.

I would like to special thanks to the thesis committee and external member for time and invaluable comments. This thesis would not be completed without your constructive suggestions.

I own my deepest gratefulness to all members in the lab at pharmaceutical and cosmetic science, Faculty of Pharmaceutical Science and nanolab at Mechanical Department, Faculty of Engineering, Chulalongkorn University for giving their special time and great advice to this research and study.

I am truly many thank you to my many colleagues who supported me with sincere comments and encouragement. Thank you my best group “Pariah”, especially KATE, for giving their encouragement to me. Thanks p’Pair, Nut, Khimook and Ble for their support and helping me in every time. I would like to apologize if I do not write any colleague name in here but please know that I would never forget you.

Above all, I extend me endless gratefulness to my beloved family and relatives for love, understanding, support and encouragement that fully inspire me to fulfill this thesis.

CONTENTS

Page

LIST OF TABLES

LIST OF FIGURES

Page

LIST OF ABBREVIATIONS

%	percentage
μg	microgram (s)
μL	microliter (s)
μM	micromolar
°C	degree celsius
CV	coefficient of variation
DI water	distilled water
FD	fluorescent
g	gram (s)
kg	kilogram (s)
L	liter
M	molar
Min	minute (s)
mL	milliliter (s)
mM	millimolar
MPa	megapascal
N	Newton
Pa	pascal
SD	standard deviation
UV	ultraviolet

CHAPTER I
INTRODUCTION

Gamma-aminobutyric acid (GABA) is a non-protein amino acid. GABA is one of neurotransmission agents which can inhibit over-stimulation of the brain and reduce hypertension from stress (Takahashi, Sumi, and Koshino, 1961; Mody et al., 1994; Hayakawa et al., 2004). GABA is generally found in human such as in the cortex, hippocampus, hypothalamus and central nervous system (CNS) (Roberts and Frankel, 1950); in animals (Awapara et al., 1950), in plants (Varanyanond et al., 2005; Ishikawa et al., 2009) and in food (Diana, Quílez, and Rafecas, 2014). GABA has a median lethal dose (LD_{50}) more than 5 g/kg when tested in rats by intravenous injection (Corneliu, 1968) and has been used to relieve insomnia and anxiety (Abdou et al., 2006; Amihăesei and Mungiu, 2011). GABA also showed some benefits to the skin. GABA showed more effect on stimulating collagen synthesis in normal human buccal mucosa when compared to arecaidine (Scutt, Meghji, and Harvey, 1987). Additionally, GABA enhanced fibroblast synthesis in hairless mouse's epidermis after tape stripping and prevented mouse from the epidermal hyperplasia which was induced by acetone treatment under low environmental humidity (Denda et al., 2002). Moreover, GABA inhibited the expression of proinflammatory mediators such as tumor necrosis factor alpha (TNF-α), interleukin-1 beta (IL-1β) and inducible nitric oxide synthase (iNOS) induced by lipopolysaccharide in NIH3T3 cells. For injured Sprague-Dawley rats, GABA treatment also suppressed inflammation and stimulated re-epithelialization resulting in speeding up of the healing process at the same rate as epidermal growth factor (EGF) (Han et al., 2007).

A potential role(s) of GABA in human dermal fibroblasts was examined by Ito et al. (2007) through the function of glutamate decarboxylase (GAD) in skin. GAD is GABA-synthesizing enzyme presented in 2 isoforms; GAD65 and GAD67 (Soghomonian and Martin, 1998). Generally, GAD65 is found in pancreatic β cells while GAD67 is found in brain tissues but little is known about non-neuronal tissue expression. Ito et al. (2007) evidenced that GAD67 mRNA and protein were

expressed in mouse skin and in human dermal fibroblasts. GAD67 localized in the dermis was shown to involve in variety of skin activities. Lower levels of hyaluronic acid (HA) and collagen were found in the knocked down GAD67 mouse. This result was in accordance with the study showing that GABA simulated the synthesis of HA by more than 2 folds as compared to the control and also increased the viability of dermal fibroblasts against oxidative stress when treated with hydrogen peroxide (H_2O_2).

In term of strengthening skin barrier, GABA was able to up-regulate human beta-defensin-2, which is an anti-microbial peptide found in the local epithelial defense system of the skin. GABA also increased gene expressions of the human hyaluronan synthase 1 (HAS1) and filaggrin (FLG) which play a role in normal barrier function of the skin. Consequently, GABA can possibly be a new strategy for anti-microbe therapy and rejuvenating skin in cosmetics (Di Cagno et al., 2010).

GABA provides many benefits to the skin as mentioned above; therefore, it will be chosen as a model drug in this study. However, GABA is a small amino acid and easily dissolves in water, delivery of GABA into the skin is challenging. Log $P_{(octanol/water)}$ of GABA equals to -3.01 (Yunger and Cramer, 1981) presenting that the penetration of GABA through the skin could be a problem. Moreover, the target sites of action could be in the viable epidermis and dermis layers. Conventional formulations may not be effective enough to deliver GABA to its target sites. SC not only is a natural barrier of human's skin but also is one obstacle to skin delivery of drug or active ingredient. To bypass the SC, microneedles are used to overcome this hindrance. Nowadays, microneedles are widely used in cosmetics. For instance, ascorbic acid (vitamin C) and retinyl ratinoate were encapsulated in hyarulonic acid dissolvable microneedles used for diminishing winkle on patients' face with no allergy or irritant (Kim et al., 2014). Additionally, microneedles were used to improve skin delivery of short peptides such as lysine-threonine-threonine-lysine-serine (Mohammed et al., 2014) and Glycyl-L-histidyl-L-lysyl (Li et al., 2015) which both stimulate collagen synthesis in the dermis. Halve dose of 5-aminolevulinic acid (a photosensitizing drug) could be successfully used to delivery drug in the skin by using polymer microneedles when compared with using cream formulation for the medication of patients who suffered from superficial basal cell carcinoma, Bowen's

disease or actinic keratoses without causing more pain (Mikolajewska et al., 2010). In conclusion, microneedles showed promising results to deliver a small amino acid into the skin.

Microneedles can be categorized into 2 types which are dissolvable and non-dissolvable microneedles. Dissolvable microneedles have been developed to completely dissolve in the skin and do not leave any waste while the drug or active ingredient is encapsulated inside the microneedles. Although there are many applications of these dissolvable microneedles, some stability problems including both physical and chemical instabilities could be found. For example, drug loading could reduce a mechanical strength of microneedles or drug may be lost, especially proteins and peptides, during the fabrication process involving heat. Dissolving microneedles prone to be sensitive to moisture; thus, the manufacturing and storage could be difficult (Kolli and Banga, 2008; Donnelly, Morrow, et al., 2009; Hiraishi et al., 2013). Alternative non-dissolvable microneedles may be preferred in some cases.

Novel fabrication process of microneedles using plastic materials was invented by Assistant Professor Dr. Werayut Srituravanich, Department of Mechanical Engineering, Chulalongkorn University. Attaining microneedles have a special shape with pocket at the tip of each needle (unpublished data). Newly invented microneedles may provide extra benefits over conventional solid microneedles including simple manufacturing, one-step application, and drug loading pockets which are available in different pocket sizes and applicable for both hydrophilic and hydrophobic drugs. Thermoplastics have been widely used in medical devices because it provides good mechanical strength and excellent physical stability when compared to dissolvable microneedles. Moreover, closed-drug pocket when being inserted into the skin allows spontaneous drug diffusion without application force unlike hollow microneedles. Drug will be loaded after fabricating microneedles; therefore, drug will not influence microneedles properties as well as drug will not be degraded by heat used during the process. Polypropylene (PP) will be chosen as plastic material because it has been used in medical devices such as disposable hypodermic syringes and sutures and it is considered safe (McKeen, 2014; Sastri, 2014).

Needle size can influence the pocket size and microneedle diameter; for this reason, different sizes of sewing needles will be selected to produce a 6 x 7 array master mold. Microneedle's height and diameter showed effects on their strength used to pass through the skin (Yan et al., 2010; Kochhar et al., 2013) as well as on the level of pain (Kaushik et al., 2001; Gill et al., 2008; Torezan et al., 2013). For instance, 300 microns microneedles were too short to pass through the skin (Verbaan et al., 2007); consequently, an applicator was needed to facilitate skin penetration of small sized microneedles (Verbaan et al., 2008). Furthermore, microneedles with more than 1000 microns in height could be painful for a patient (Gill et al., 2008). Regarding to our preliminary study, 1000 microns microneedles could be fabricated by this technique. Balancing between delivery the drug deep into the target sites which are viable epidermis and dermis layers and do not cause any pain, press force will be studied to obtain the optimum penetration distance with this microneedle size. Various dipping distances will be studied to generate different pocket sizes and may consequently result in different drug loadings. Moreover, failure strength test will be performed to determine a maximal force causing needle deformation or fracture.

On the other hand, Small amino acid, like GABA, is shortly eluted with solvent front in standard analytical method. In addition, GABA does not have fluorescent or strong ultraviolet (UV) absorbance characteristics (Shah, Crespi, and Heidbreder, 2002). Thus, analysis of GABA requires derivatization to prolong GABA retention time and provide strong UV and fluorescent absorbance. Developed analytical methods have been reported using several derivatizing agents including phenylisothiocyanate (PITC) (Jarry et al., 1992), 2-hydroxynaphthaldehyde (HN) (M. Y. Khuhawar and A. D. Rajper, 2003), 4-dimethylaminoazobenzene-4-sulfonyl chloride (DABSYL-Cl) (Varanyanond et al., 2005), naproxen acyl chloride (NAC) (Hsieh, Tsai, and Wu, 2006), 1-fluoro-2,4-dinitrobenzene (FDNB) (Ishikawa et al., 2009) and o-phthaladehyde (OPA) with 3-mercaptopropionic acid (MPA) (de Freitas Silva, Ferraz, and Ribeiro, 2009). Different derivatizing agents showed differences in sensitivity and some derivatives degraded quickly which may cause some difficulty in GABA analysis. Therefore, two derivatizing agents, HN and OPA with MPA, will be compared in terms of sensitivity and derivative stability. Additionally, comparative

validation results will provide information that will be used to choose the derivatizing agent in a specific test such as drug release or skin permeation study.

The objectives of this study are to develop novel fabricating polypropylene microneedles containing GABA, to study effect of dipping distances on physical properties of microneedles (e.g. pocket size, fraction force, skin penetration, and drug loading) and to compare two GABA HPLC analytical methods using 2-hydroxynaphthaldehyde (HN) or o-phthaladehyde (OPA) with 3-mercaptopropionic acid (MPA) as derivatizing agent

CHAPTER II
LITERATURE REVIEW

1. Structure and properties of skin and its components

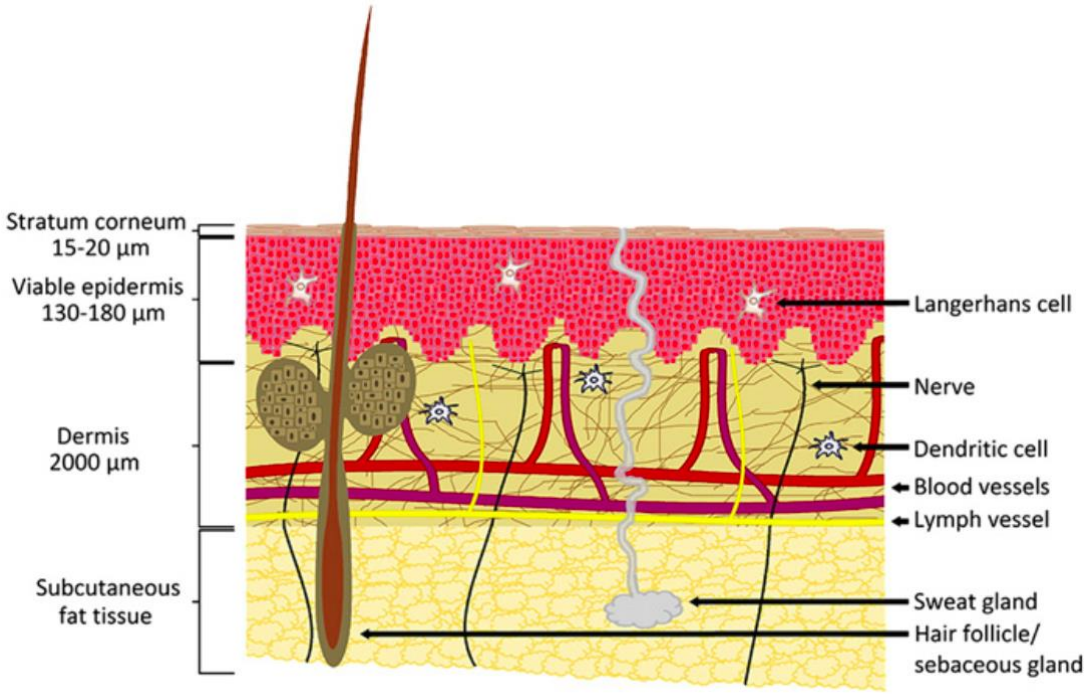

Figure 1 The human skin structure (van der Maaden, Jiskoot, and Bouwstra, 2012)

There are three main layers of human skin, which are epidermis, dermis and subcutaneous layer as shown in figure 1. The outer layer, epidermis, can be divided into four parts. The first part is the non-viable epidermis, stratum corneum (SC), which has 8-20 µm thickness. The second part is viable epidermis, 30-200 µm thick. This part is composed of three composites which are stratum granulosum, stratum spinosum and stratum basale, respectively. The middle layer is dermis, which is 500-5,000 µm thick. Dermis can be divided into two parts, papillary and reticular dermis. The last layer is subcutaneous tissue. Additionally, the thickness of each layer's skin is varied on ages, genders and individuals (Anderson and Parrish, 1982; Kenneth and Michael, 2002; Agache, Agache, and Humbert, 2004; Magnus and Bo, 2005; Archer, 2010; McGrath and Uitto, 2010).

SC is composed of corneocytes surrounding by intercellular lipids which are ceramides, cholesterols and fatty acids. It is responsible for a physical barrier effect. With this effect, SC prevents the loss of water and electrolytes from the skin. Additionally, the skin has a mechanism to maintain a balance of water in SC by filaggrin. Filaggrin (FLG) is produced from profilaggrin, in which its by-product is called natural moisturizing factors (NMF). NMF is amino acids and their derivatives can be found in two major substances, which are pyrrolidone carboxylic (PCA) and trans-urocanic acid (UCA). NFM is water-soluble and hygroscopic molecule which becomes a potential humectant in SC. Laden (1967) discovered that NMF existed in human SC. People having a mutant FLG gene were found to have less NMF in forearm and palmar skin (Kezic et al., 2008). In addition, NMF was found to have a relationship with a hydration in SC, where a low level of NMF was related to a low level of water in SC (Katagiri et al., 2003; Bouwstra et al., 2008). In the lowest layer, viable epidermis consists of keratinocytes originated from stratum basale that involves in proliferation and differentiation of keratinocytes.

On the second part of skin, dermis is the major part of human skin. Primary functions of dermis are to support against external force, provide elasticity and nutrients, and maintain thermal regulation and hydration to the skin. Dermis layer mainly composes of collagen fibers (70%) and glycosaminoglycans (GAGs). GAGs are highly charged polyanionic molecules which attach to the core protein. Hyaluronic acid (HA) is disaccharide polymer with repeating of D-glucuronic acid and N-acetylglucosamine. In human skin, HA is produced by hyaluronan synthase (HAS). Several HASs were found in epidermis; HAS3 and particular HAS1 (Sayo et al., 2002), and in dermis; HAS1 and HAS2 (Sugiyama et al., 1998). HA was found to play important roles in water homeostasis, being space-filling molecule, providing elastic and cushioning properties in the dermis (Cleland and Wang, 1970; Laurent, 1987; Scott et al., 1991). HA has been used in many fields. In the medical field, HA combining with iodine complex helped to treat a foot ulcer or wound (Sobotka et al., 2007; Brenes et al., 2011). Moverover, topical gel formulation of 2.5% HA with 3% diclofenac was used in a treatment of actinic keratoses (Wolf et al., 2001). In the cosmetic field, HA cream was formulated and found to improve skin hydration and elasticity (Pavicic et al., 2011). Furthermore, HA could facilitate transdermal delivery

when using as a carrier in nanoemulsion (M. Kong et al., 2011). There by, FLG and HA are the two major substances which play an important role to firm and hydrate the skin.

2. GABA and Benefits to skin

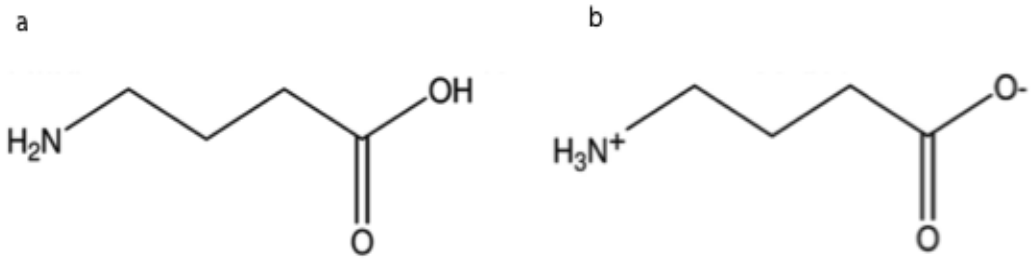

Figure 2 The structure of neutral (a) and zwitterionic (b) GABA (Jiang, Fu, and Zhang, 2010)

Gramma-aminobutylic acid (GABA) as presented in Figure 2 is synthesized by glutamate decarboxylases (GAD); GAD65 and GAD67 in human. Ito et al. (2007) found that GAD 67 existed in BALB/c, HR-1 and C3H/HeN mice more than GAD 65 and also found GAD67 in human dermal fibroblast. Moreover, knocked down GAD 67 mice exhibited lower in dermis thickness than that of the normal mice without changes in epidermis thickness (Ito et al., 2007). Furthermore, low amounts of collagen fibers or HA could result in thinner dermis. Besides, 10 μg/mL GABA could increase collagen synthesis in normal human buccal mucosa fibroblasts (Scutt, Meghji, and Harvey, 1987). Moreover, 1 μg/mL GABA could significantly stimulate 2-fold HA synthesis in human dermal fibroblast but no effect on collagen synthesis in the same model (Ito et al., 2007). In addition, dermal fibroblasts treated with 1 μg/mL GABA were exposed to hydrogen peroxide (H_2O_2) in a stress condition, significantly higher cells viability and glutathione synthesis were found compared with untreated GABA (Ito et al., 2007). Therefore, GABA could be produced in dermis and 1 μg/mL GABA could increase HA synthesis and involve in anti-oxidation by up-regulating glutathione in dermis fibroblasts (Scutt, Meghji, and Harvey, 1987; Ito et al., 2007).

In regards to wound healing and inflammatory, Han et al. (2007) found that 10 μM GABA could significantly stimulate cell proliferation in mouse fibroblasts (NIH3T3). At the same concentration, GABA inhibited pro-inflammatory mediators such as inducible nitric oxide synthase (iNOS), interleukin-1 beta (IL-1β) and tumor necrosis factor-alpha (TNF-α) in lipopolysaccharide (LPS) induced inflammation mouse macrophage RAW 264.7 cells (Han et al., 2007). iNOS is a nitric oxide synthase found in human body. It produces nitric oxide (NO), a signaling molecule, which provides regulations of vascular system and stimulation of immune system. On the contrary, NO can turn into free oxygen radical ($NO^{\cdot}$), acting as a cytotoxic agent, which involves in inflammatory disorders like psoriasis (Sirsjö et al., 1996; Bruch-Gerharz, Ruzicka, and Kolb-Bachofen, 1998; Aktan, 2004). IL-1β is a cytokine that induces body sensitivity to infection such as auto-inflammatory diseases (Feldmeyer et al., 2010; Lane and Lachmann, 2011). TNF-α is also a cytokine, which acts as a pathogenic mediator causing an inflammation in the skin (Tracey and Cerami, 1994; Groves et al., 1995).

Han et al. (2007) also found that on the 5^{th} day of 10 μM GABA treatment, collagen and fibroblast fibers were increased in the male adult Sprague-Dawley rats' back and were comparable with 100 μL epidermal growth factor (EGF) treatment. EGF is a 53-amino acid polypeptide which helped speed the healing process of wounds (Brown et al., 1989; Nanney, 1990). In addition, the GABA treatment also significantly up-regulated the expressions of platelet-derived growth factor (PDGF) and transforming growth factor-β (TGF-β) on the 5^{th} day post wounded (Han et al., 2007). PDGF is a serum growth factor polypeptide which stimulates fibronectin and glycosaminoglycan (GAG) synthesis (Pierce et al., 1992; Andrae, Gallini, and Betsholtz, 2008). Another factor, TGF-β is a polypeptide cytokine, which triggers GAG, fibronectin and collagen (Pierce et al., 1992; Faler et al., 2006) through other pathway (Pierce et al., 1989). Hence, 10 μM GABA would be beneficial to the wound in terms of fast-promoting wound healing and reduction of pro-inflammatory mediators.

In term of improving healthy skin, 0.86 mM GABA could stimulate the highest expression of human beta-defensin-2 (HBD-2) gene after 48 hours in SkinEthic® Reconstructed Human Epidermis by RT-PCR confirmed by

immunohistochemical analysis (Di Cagno et al., 2010). HBD-2 is a cysteine-rich cationic peptide and is produced at low level under normal skin condition (Harder et al., 1997; Chadebech et al., 2003). It was up-regulated in the inflammatory skin or was induced by bacteria such as Gram-negative bacteria and *Candida albicans* except Gram-positive *Staphylococcus aureus* (Schröder and Harder, 1999). Additionally, Di Cagno et al. (2010) found that 0.86 mM GABA increased the expressions of HAS 1 and filaggrin genes in the multi-layer human skin model (FT-skin) tissue detected by RT-PCR after 24 hours and 72 hours of the treatment, respectively. Additional, ELISA analysis was also performed on the same samples and showed high levels of hyaluronic acid and filaggrin protein after 24 hours and 72 hours of the treatment, respectively, in which the result was in agreement with RT-PCR study. Therefore, 0.86 mM GABA showed interesting effects on improving skin barrier and firming skin. However, GABA is expected to have difficulties in getting to target sites in viable epidermis and dermis because of its small-water-soluble molecule. So, it is not easy to deliver GABA through the hindrance.

3. Skin delivery of small amino acid

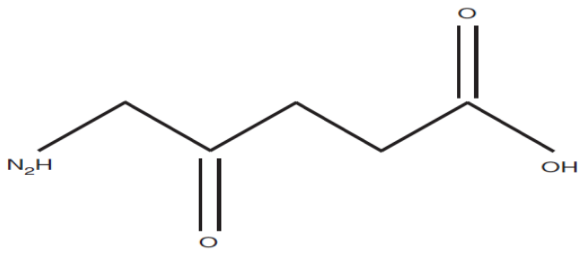

Figure 3 The structure of 5-ALA (Kormeili, Yamauchi, and Lowe, 2004)

5-aminolevulinic acid (5-ALA) is an amino acid as shown in Figure 3 and a prodrug used in photodynamic therapy (PDT) for skin cancer treatment. 5-ALA is a precursor of the photosensitizer protoporphyrin IX (PpIX). PpIX is generated in heme biosynthesis. This photosensitizer can be activated by specific wavelength light to produce singlet oxygen as cytotoxic free radicals, which can kill exposed cells. However, 5-ALA is a water-soluble and small molecule similarly to GABA. Thus, SC is a primary barrier to deliver 5-ALA to the target area of viable epidermis or dermis depending on the symptom. One of the most successful methods used to deliver 5-

ALA to the skin is microneedles (MNs). MNs are a minially invasive puncture with no pain or bleeding. According to Donnelly et al. (2008), 5 hours after applying of silicon MN arrays (or 19 mg 5-ALA cm^{-2} patch) showed an increase in 5-ALA with a mean flux enhancement ratio of 2.39 across normal murine skin. The studied MNs were 270 μm in height, 240 μm in diameter of the base and 750 μm in an interspacing between rows. In clinical trial, biodegradable polymer MNs containing 2 %, 8 % and 16 % of 5-ALA were successfully delivered 5-ALA through the SC and found that 8 % and 16 % 5-ALA gave similar PpIX inductions after incubation for 4 hours. Moreover, these MNs were 600 μm in height, 300 μm in width, 300 μm in each interspacing and 121 microneedles per centimeter square, which did not report pain and erythema during and/or after the treatment (Mikolajewska et al., 2010).

For cosmetic uses, 32 % retinyl retinoate and 33% ascorbic acid were loaded into dissolvable HA microneedles. Loaded HA microneedles, which had 153 needles, 220 μm in length and 30 μm in tip could reduce skin's wrinkle and roughness after 12 weeks treatment with no allergic and significant side effects to patients (Kim et al., 2014). In addition, stainless steel MNs, which had 3 needles with 700 μm in length and 250 μm in width, helped small peptides such as pal-KTTKS to pass into SC after applying MNs (Mohammed et al., 2014). Additionally, a plastic microneedle patch consisting of 351 needles with 700 μm in height and 500 μm in a tip-to-tip needle spacing were used to pretreat human skin with 22.2 N force before applying of peptide GHK and Cu treatments. Then, 134 nM of peptide GHK and 705 nM of Cu were found in the skin at 9 hours after pretreatment; therefore, MNs helped improve skin delivery of those drugs (Li et al., 2015). As a consequence, a water-soluble and small molecule such as amino acid or short peptide were successfully delivered through the viable epidermis and dermis by the aid of MNs. Therefore, MNs might also possibly deliver GABA to its targets successfully.

4. Microneedles

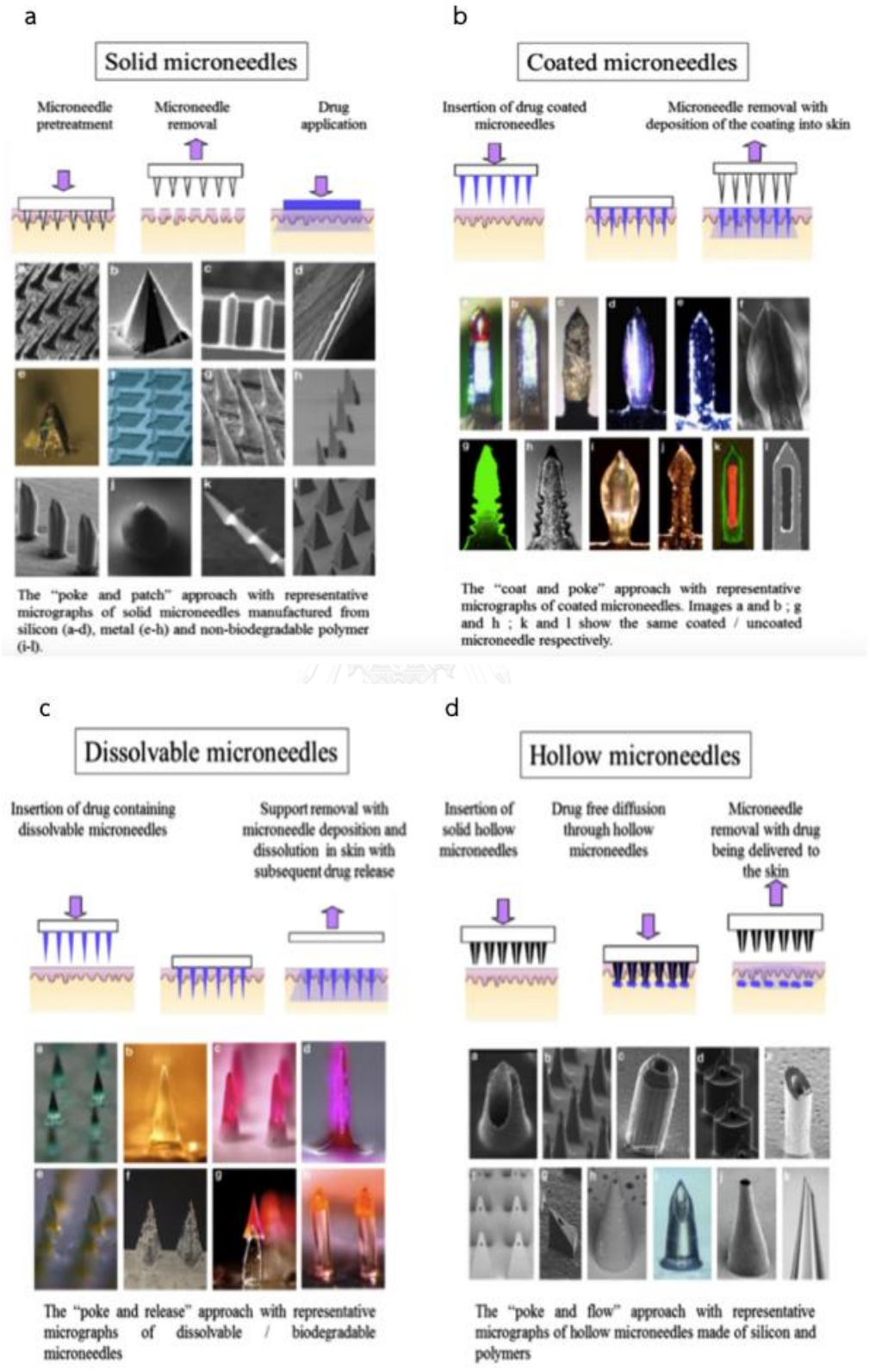

Figure 4 Types and general applications of MNs: solid MNs (a), coated MNs (b), hollow MNs (c) and dissolvable MNs (d) (Gratieri et al., 2013)

As mentioned above, MNs application is a minimal invasive means, which reduces pain and is easy to use. Moreover, Donnelly, Singh, et al. (2009) noted that microneedles were likely to have lower risk of healthcare-associated infection when comparing with using of hypodermic needles. MNs can be generally categorized into two groups, which are dissolvable and non-dissolvable microneedles. In addition, they can also be classified into four types depending on how to use microneedles shown in Figure 4. The first type is called "Poke and Patch" which MNs are made of solid materials such as silica or stainless steel. There is a two-step application. First, the targeted skin area will be pierced by microneedles to create micropore channel. Next, a conventional formulation including gel, solution or cream with loaded drug(s) will be applied to the targeted area (Lin et al., 2001; Martanto et al., 2004). The second type, coated microneedles or called "Poke and Coated", is solid microneedles in which drug(s) or active ingredient(s) is/are coated on the surface of microneedles. These MNs will release drug(s) or active ingredient(s) into the skin after insertion (Gill and Prausnitz, 2007b, 2007a). The third type, hollow microneedles or called "Poke and Flow", has one or more pores in the needle's platform. Also, some pressure pump or injector might be used to flow a liquid formulation through the skin during the treatment (Gardeniers et al., 2003; Martanto et al., 2006; Wang et al., 2006). Furthermore, these three types are usually non-dissolvable MNs which have several advantages including short application time, short time of production and using low-cost fabrication material.

The last type of MNs, dissolving microneedles or called "Poke and Release", has been developed to be dissolved completely in the skin and it will not leave any residue after using. This MNs type is made of safe, water-soluble and biodegradable material(s) such as polymers or sugars (Park, Allen, and Prausnitz, 2005; J. W. Lee, Park, and Prausnitz, 2008; Donnelly, Morrow, et al., 2009; Martin et al., 2012; Hiraishi et al., 2013). Drug(s) or active ingredient(s) is/are encapsulated inside the microneedles. Unfortunately, drug loading could reduce a mechanical strength of microneedles and/or could have drug stability problem after being incorporated in dissolving microneedles. Moreover, drug loss was also occurred due to the fabrication process or material of MNs' backbone (J. W. Lee, Park, and Prausnitz, 2008; Donnelly, Morrow, et al., 2009; Hirobe et al., 2013). Regarding to the mentioned

drawbacks, a new innovative MNs will be developed to overcome the drawbacks of currently available MNs.

5. An innovative microneedles

Figure 5 The animation of innovative miconeedles

Referring to Assistant Professor Dr. Werayut Srituravanich, Department of Mechanical Engineering, Chulalongkorn University, who invented a new fabrication of MNs using plastic materials, the new MNs have a new shape with auto-generated pocket at the tip of each needle (unpublished data) presented in Figure 5. This novel modified MNs shall provide additional benefits over typical hollow MNs in terms of driving force of drug into skin. After applying this novel design on to the skin, the drug in the pocket will get dissolved by skin water which facilitated by occlusive effect of the MNs patch and then will diffuse into the skin by concentration gradient. Unlike typical hollow MNs with 2 open-ends, after applying drug could get dried out and/or a use of applicator such as syringe may be required to push the drug into the skin. Moreover, this newly designed hollow MNs are made of plastic which provides high robustness in fabrication process than other materials used in dissolving MNs. Chosen plastic has sufficient strength and is medical grade which previously used in medical devices. In this present study, a 6x7 array's master mold consists of 42 microneedles per one patch. About the type of fabrication material, polypropylene (PP) plastic was chosen as a plastic model because it has been used in medical devices such as disposable hypodermic syringes and sutures and it is considered safe (McKeen, 2014; Sastri, 2014). Furthermore, the PP is available in pharmaceutical grade, easy to purchase and not expensive. Thus, polypropylene MNs were cast in this study in order to deliver GABA to the skin.

About the first studied factor, the height of MNs was known to associate with the amount of pain to patients while using MNs. According to Kaushik et al. (2001), 12 healthy patients were treated with 400 silicone MNs with 150 μm height on their arms and they did not feel pain. Moreover, stainless steel MNs with 480, 700, 960 and 1,450 μm height caused less pain than the 26-gagaue hypodermic needle in the study of 10 healthy volunteers tested on their volar forearms (Gill et al., 2008). MNs' height was directly correlated with the pain, where longer MNs would cause more painful to the patient. Small blood droplet was found after inserting the MNs with 1450 μm in height while a sign of bleeding was always found after inserting the hypodermic needle (Gill et al., 2008). Therefore, the height of MNs should be less than 1450 μm to prevent bleeding after applying MNs. On the other hand, Verbaan et al. (2007) found that metal MNs in 300 μm height could not successfully penetrate dermatome human skin while MNs with 550, 700 and 900 μm in height could penetrate the skin effectively and also improved the delivery of a compound with MW of 72 kDa after pretreatment of MNs. Same research group (Verbaan et al., 2008) using an applicator with metal 300 μm-MNs could successfully penetrate the skin with an extra of applied velocity and also resulting in better performance. Not only too short MNs (i.e., 300 μm-metal MNs) but also hollow MNs could be used with an applied velocity of 1 m/s or 3 m/s applicator to improve skin penetration of those MNs. More consistent drug delivery could also be obtained from short MNs applied by an applicator.

Moreover, silica MNs, having more than 600 μm in height, increased the delivery of acyclovir through the human epidermal membrane (HEM). Acyclovir is a water-soluble and small molecule with MW of 225.21 Da; therefore, it would have difficulty getting into the intact skin (Yan et al., 2010). MNs' height showed an influence on MNs' performance including degree of pain after poking as well as poking efficiency. Consequently, MNs with 1 mm in height was chosen to deliver GABA regarding to the results from previous studied and it was expecting to be safe, less painful and do not cause any bleeding.

Another studied factor is the dipping distances. Different dipping distances; 1 and 1.5 mm in this present study, could provide different auto-formed pocket sizes. As a consequence of different pocket sizes, different GABA amounts could be loaded

into the pocket. Which later, the dipping distance can be used to tailor-make to serve different needs.

6. The evaluation of physical and chemical properties of polypropylene microneedles loaded GABA

Generally, physical and chemical properties are considered in all types of delivery systems. For physical property of MNs, MNs are normally evaluated in terms of mechanical property using fracture force test against a hard surface such as aluminum or stainless steel and skin insertion by piercing across soft surface such as animal or human skin. To obtain MNs that can be used in human, MNs have to be strong enough not to break inside the skin and can be inserted to the skin.

Firstly, failure strength test is the test to determine the strength of MNs and is presented as the plot between applied force (N) on MNs and displacement (mm) or a decreasing movement on axial distance. The critical point or called "failure force point" is the maximum applied force before the sudden drop in force. The failure force point represents the maximum force that MNs can withstand before going to deform or fracture as presented in Figure 6.

For example, poly (lactic-co-glycolide) (PLGA) with 700, 1000 and 1500 μm height and 200 μm base diameter showed failure force points in the range of 0.1-0.22 N/needle using the displacement of 1.1 mm/s (Park, Allen, and Prausnitz, 2005). Following work, the conical PLGA MNs with 500 μm height and 200 μm base diameter could withstand more force with fracture force point of 0.4 N/needle under the same test conditions (Park and Prausnitz, 2010). This research group suggested that the shorter MNs and conical shape could be stronger than the longer MNs.

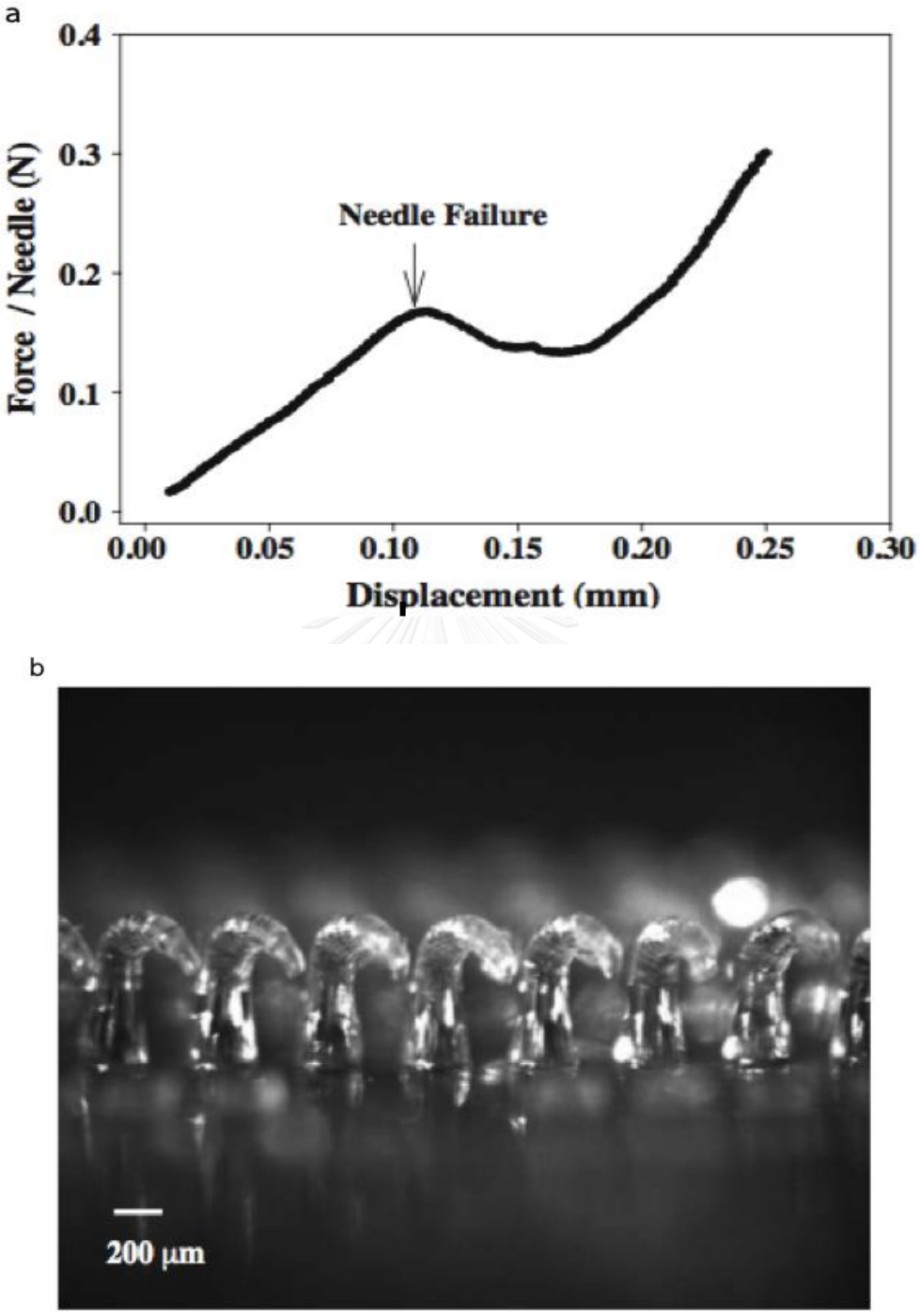

Figure 6 The graph (a) and light micrograph (b) of polymeric MNs after failure strength test (Park, Allen, and Prausnitz, 2005)

Moreover, carboxy-methylcellulose (CMC) MNs with 500 μm height, and 300 μm base width withstood the force at 0.5 and 0.1 N/needle for the pyramid shape and the conical shape, respectively, in the fracture force test using the displacement of 1.1

mm/s (J. W. Lee, Park, and Prausnitz, 2008). It could be concluded that MNs shape affected on the fracture force of MNs. Casting material also showed an influence on the fracture force, for example, MNs casted with a copolymer methylvinylether and maleic anhydride (PMVE/MA) (a conical shape, 600 μm height and 300 μm base width) showed the fracture force of 0.711 N/needle using the displacement of 1.1 mm/s (Donnelly et al., 2011). Thus, PMVE/MA MNs gave the maximum fracture force among the dissolvable MNs. Whereas, non-dissolvable MNs were likely to have higher fracture force than a dissolvable group. For an example, nickel conical hollow MNs with 500 μm height and 300 base width were reported to have fracture force of 3 N/needle. Hollow metal MNs with 150 μm outer tip radius and 37.5 μm inner tip radius required an insertion force about 0.2 N/needle to insert MN into human skin (Davis et al., 2005). Additionally, ceramic MNs with 300 μm height and 100 μm diameter had a fracture force of 1.62 N/needle(Bystrova and Luttge, 2011). Therefore, non-dissolvable MNs are generally strong enough to penetrate the skin without fracture compared with dissolvable MNs.

Secondly, MNs not only insert without fracture but also penetrate successfully through the skin. The standard model, which is used to evaluate skin penetration, is human skin. However, it is not easy to acquire human skin, so using an animal skin is an alternative choice to perform the efficacy of MNs. The pig skin has been a preference over many years because of its similar thickness to the human skin. Thus, successful piercing to the pig skin could be good prediction of piercing ability when being used with the human skin as shown in Figure 7 (Godin and Touitou, 2007; Barbero and Frasch, 2009).

The pyramid CMC MNs with 600 μm height and 300 μm base width penetrated into cadaver pig skin after using a thumb press at 1.5 N within 3 seconds. The approximate penetrated depth was 150-200 μm thick (J. W. Lee, Park, and Prausnitz, 2008). Additionally, galactose MNs arrays with 270 μm height and 240 μm base diameter were pressed against piglet epidermis at a speed of 0.5 mm/s for 30 seconds with gradually increasing known forces from 0.05 to 0.267 N/MN. With applying force of more than 0.2 N/needle, over 90% of the MNs in the array were shown to puncture piglet epidermis (Donnelly, Morrow, et al., 2009).

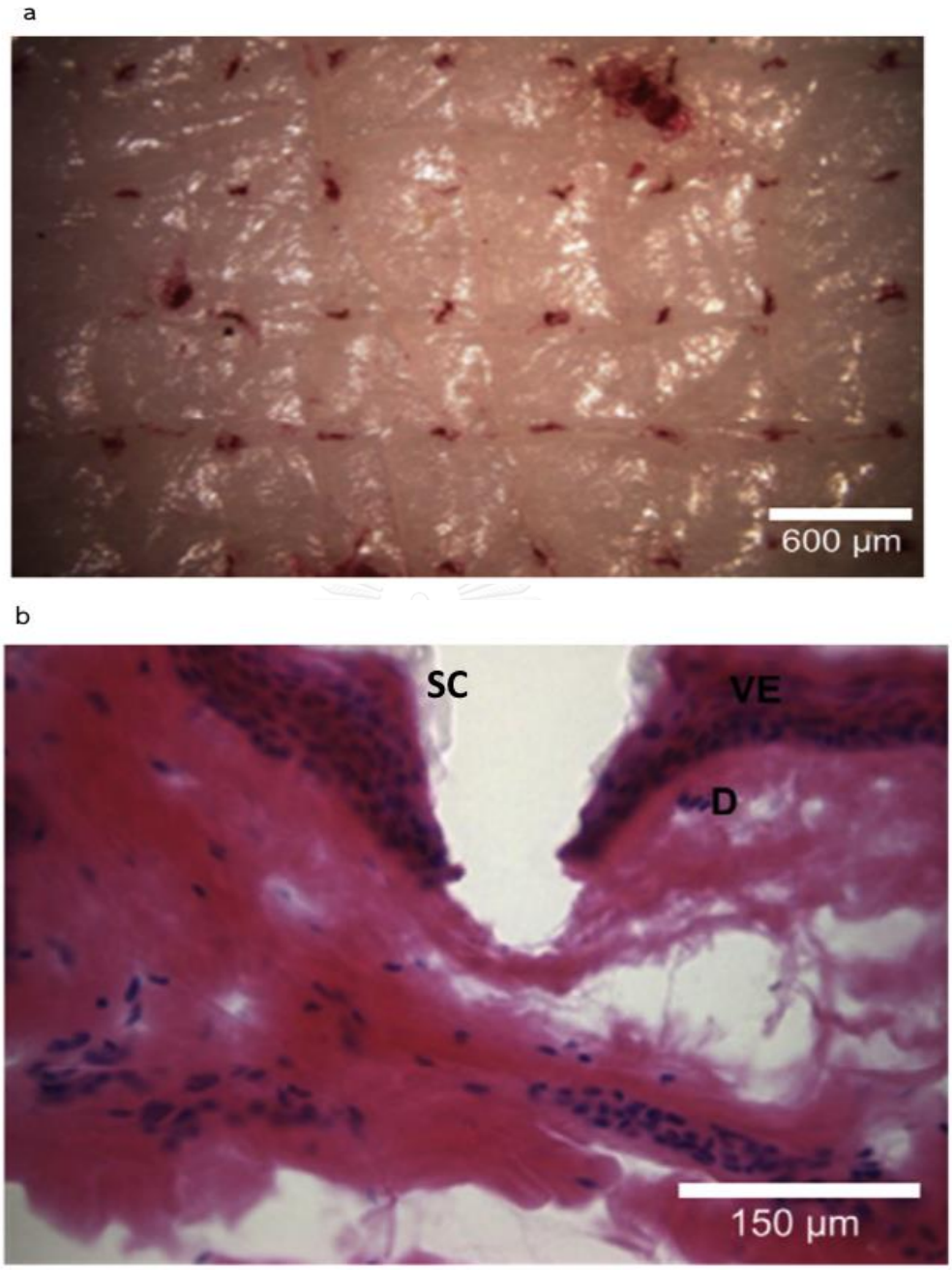

Figure 7 Skin stained with dye to identify MNs penetration after insertion of polymeric MNs (a) and cross-sectional image of H&E stained skin at site of MNs penetration (b) (SC: stratum corneum, VE: viable epidermis and D: dermis) (J. W. Lee, Park, and Prausnitz, 2008)

For PMVE/MA MNs with 600 µm height and 300 µm base width, the majority of MNs in an array penetrated the stratum corneum of neonate porcine skin when the insertion force was 0.03 N per MN or greater (Donnelly et al., 2011). Olatunji et al. (2013) performed the MN insertion force into excised neonatal porcine

skin. By increasing insertion speed from 0.5 to 1.0 mm/s, insertion force values were decreased from 0.03 to 0.0216 N for 30 μm interspacing at MNs base (300 μm interspacing at tip). From these reviews, the height of MNs may not be only factor influencing on the required force for skin insertion but both insertion speed and interspacing between needles also showed an influence.

With the innovative MNs design including an auto-formed pocket, drug loading should also be evaluated to show how much drug solution could be loaded into very small cavity by capillary force. The influence of dipping distance could also be studied by analyzing the drug content. There are several methods which have been used to detect the amount of GABA. High-performance liquid chromatography (HPLC) is considered as a standard analytical method because of simplicity, sensitivity, reproducibility and economics. However, small amino acid, like GABA, is shortly eluted together with solvent front when using the standard HPLC. In addition, GABA did not have fluorophore or strong ultraviolet (UV) absorbance characteristic (Shah, Crespi, and Heidbreder, 2002); thus, derivatization using derivatizing agents may be required to prolong GABA retention time and to provide strong UV or fluorescent absorbancy in the analysis of GABA.

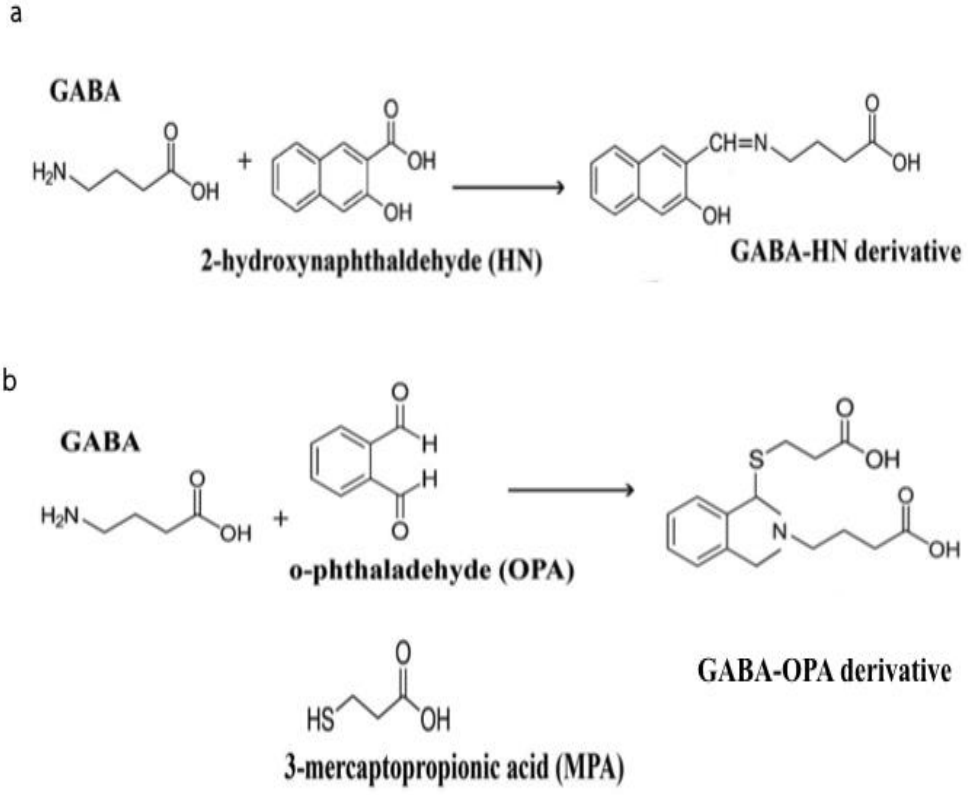

Figure 8 The reaction scheme of GABA+HN (a) and GABA+OPA with MPA (b) derivatives

Normally, derivatizing agents have their own efficiency and affinity which differently interact with amino acids. The reported derivatizing agents which were used to analyze amines are 2-hydroxynaphthaldehyde (HN) (Mañes et al., 1988; Mohammed El-Brashy and Mohammed Al-Ghannam, 1997) and o-phthaladehyde (OPA) binding primary amine (K. S. Lee and Drescher, 1978; Cronin, Pizzarello, and Gandy, 1979), 4-dimethylaminoazobenzene-4'-sulphonyl chloride binding primary and secondary amine (Handley et al., 1998) and 2-naphthyl chloroformate binding tertiary amine (Gübitz, Wintersteiger, and Hartinger, 1981). Additionally, derivatization complexity and derivative's stability could be affected by using different derivatizing agents. For this reason, several analytical methods have been developed to provide a complete derivatization between amino acid and derivatizing agent with reproducibility and to provide a considerably stable derivative, which is feasible to be used for GABA analysis.

Several published papers revealed the studies studied about the analysis of GABA using derivatization. For an example, the derivative of GABA with OPA was unstable in acid medium (half-life ≅ 8 min) and required HPLC coupled with fluorescent detector (FLD) (Sunol et al., 1988). Another analysis of GABA in dentate gyrus (Sheng, Hang, and Ruan, 2005) and milled rice (Iwaki and Kitada, 2007) using of OPA with β-mecaptoethanol (MCE) improved the stability of the derivative. Where using OPA with 3-mercaptopropionic acid (MPA) as showed in Figure 8(b) provided the more stable derivative compared with OPA with MCE (Molnár-Perl, 2001; Devall et al., 2007). Even though, napthalene-2,3-dicarboxaldehyde (NDA) provided the most stable derivative compared with the derivative of OPA with MPA, the NDA derivative was more toxic and the process took longer incubation time than using OPA with MPA as derivatizing agents (Dawson et al., 2004; Clarke et al., 2007). In addition, de Freitas Silva, Ferraz, and Ribeiro (2009) improved the analytical method of GABA using OPA with MPA to be more rapid and easier by using an isocratic system.

On the other hand, the derivative of GABA and HN as presented in Figure 8(a), which was detected by UV detector, had a low detection sensitivity in GABA detection level but it provided more stable derivative with longer half-life than the derivative of GABA and NDA (M. Y. Khuhawar and A. D. Rajper, 2003; Hayat et al.,

2015). Therefore, different derivatizing agents showed some differences in reaction sensitivity and some derivatives were quickly degraded which may cause some difficulty in analysis. Furthermore, comparison of the two selected derivatives (i.e., HN and OPA with MPA) is also studied to provide more information for derivatizing agent selection in terms of stability and sensitivity.

CHAPTER III
MATERIALS AND METHODS

Materials

1. 2-Hydroxy-1-naphthaldehyde (HN) (Sigma-Aldrich, USA)
2. 3-Mercaptopropionic acid (MPA) (Merck, Germany)
3. 4-aminobutyric acid (GABA) (Merck, Germany)
4. Acetic acid (RCI Labscan, Thailand)
5. Boric acid (Merck, Germany)
6. Hydrochloric acid (HCl) (RCI Labscan, Thailand)
7. Hypersil BDS C_{18} (Thermo Fisher Scientific, USA)
8. Methanol (HPLC grade) (Honeywell, USA)
9. Methylene blue (Sigma-Aldrich, USA)
10. ortho-Phthalaldehyde (OPA) (Merck, Germany)
11. Polypropylene (PP) (Polimaxx, Thailand)
12. Potassium chloride (Carlo Erba, France)
13. Sodium acetate (Carlo Erba, France)
14. Sodium tetraborate (Borax) (Ajax Finechem, Australia)
15. Tetrachloroethylene (RCI Labscan, Thailand)
16. Tetrahydrofuran (RCI Labscan, Thailand)
17. Zorbax 300SB-C_{18} (Agilent, USA)

Instruments

1. Analytical balance (Mettler Toledo, Switzerland)
2. Digital microscope (Dino-lite, Taiwan)
3. High-performance liquid chromatography (HPLC) (Shimadzu, Japan)
4. Hot plate (IKA, Germany)
5. Magnetic Stand and micrometer head (Mitutoyo, Japan)
6. Micorpipette (Gilson, USA)
7. Microscope (Seek, Thailand)
8. pH meter (Mettler Toledo, Switzerland)
9. Plasma cleaner (Harrick Plasma, USA)
10. Thermometer (Fluke, USA)
11. Vacuum oven (Jeio Tech, Korea)

Methods

1. Fabrication of polypropylene microneedles

A master template consisting of 42 sewing needles was fixed into an acrylic block to obtain a 6 x 7 microneedle array master template. It was prepared for fabrication of polypropylene microneedles.

1.1 Preparation of master template

1.1.1 Sewing needle selection

The first step, sewing needles number 9 and 11 were purchased and needle widths at the distances of 0.1, 0.15 and 0.2 mm from the tip were measured in order to classify which is smaller than another. The second step, sewing needles No. 11 were chosen and evaluated for their variation in size under an inverted microscope by measuring needle widths at the distances of 1 and 1.5 mm from the tip. Mean and standard deviation (SD) were recorded. The needle was excluded when it had widths outside the range of mean ± SD at least two from three measure sites. Moreover, the selected needles must have all the widths fall within ± 10 % of each mean width.

1.1.2 Preparation of a microneedle array master template

Selected needles were fit into a 42 hole-acrylic block and then needle tips were alignied by positioning all the tips onto flat surface of a glass slide. A master template was glued using polystyrene glue and let it air-dried. Afterward a master template was finally glued with supporting platform using epoxy glue.

1.1.3 Preparation of polypropylene microneedles

The master template was attached to an adjustable stage which can be lift up and down with known distance. Aluminum block was designed to have 4 rectangular shaped templates with 3 millimeters depth by Faculty of Engineering, Chulalongkorn University to maintain the set temperature. A small petridish was attached into Al block and placed on a hot plate at the same alignment with the master mold. The tray

template together with petridish were pre-heated at 230 °C for 30 minutes. Polypropylene beads will be added into the hot tray template and kept on heating at 230 °C for 15 minutes. After that, excess plastic was removed and a surface was smoothen by the use of spatula. A master template was, then, slowly dipped into melted plastic at the predetermined distance and the system was cooled down to 180 °C for an hour. Microneedles were casted by pulling up the master template to the fixed distance. Finally, polypropylene microneedles were cooled down for 45 minutes and then, the master template was detached.

2. Characterization of GABA loaded microneedles

2.1 Physical characteristic

2.1.1 Physical appearance of polypropylene microneedles by using SEM and/or optical microscope

Scanning electron microscopy (SEM) and optical microscope were used to visualize geometry and dimensions of fabricated microneedles. Microneedle array was directly placed into a SEM without any further coating. Images were taken at various magnifications to observe the geometry, actual length, base width and tip radius of the microneedles.

2.1.2 Failure strength test

Failure strength test of polypropylene microneedles was performed to determine a maximal press force causing needle deformation or fracture using the modified method from Luangveera et al. (2015). Microneedles were attached onto a plane of a manual stage which had a weighting machine underneath. After that, the stage was slowly moved downward against microneedles with 2 small scales per 5 seconds. Applied force and displacement value were recorded. A graph of the relationship between force and displacement was presented to define a maximal press force. Afterward, SEM images of these microneedles were captured to observe any damages.

2.1.3 Skin penetration test

This study was conducted by Faculty of Dentistry, Chulalongkorn University. Skin penetration test was performed to characterize the mechanical function of microneedles. Force was applied to microneedles to achieve skin penetration depth between 600-800 micron. The method modified from Luangveera et al. (2015). Briefly, a cadaver pig skin was used as a substrate and fixed on foam. Then, polypropylene microneedles were applied by varying different forces on the skin. Microneedle tips were stained with a tissue marking dye for marking the locations of the opened holes on the skin. After that, the skin was fixed in 10 % formaldehyde for 18 hours before embedding in paraffin wax. The skin was sliced by a microtome and stained by using haematoxylin and eosin. Finally, the histology sections were examined in an optical microscope.

2.2 Chemical characteristic

2.2.1 Drug content by GABA analysis by High performance liquid chromatographic (HPLC) method

Because GABA is a small and water-soluble molecule, that makes it more difficult to quantify the amount of GABA with conventional analytical method. In this study, GABA was derivatized using 2 derivatizing agents which were 2-hydroxynaphthaldehyde (HN) and o-phthaladehyde (OPA) with 3-mercaptopropionic acid (MPA). Method validations were conducted for both derivatizing agents and later were compared under validation parameters as shown below.

2.2.1.1 HPLC Conditions

2.2.1.1.1 GABA and HN

Method was modified from M. Khuhawar and A. Rajper (2003), 1 mL GABA solution was mixed with 0.6 mL borax buffer pH 8 and 1 mL of derivatizing reagent HN (0.3 % w/v in methanol). The solution was heated on a water bath at 80 °C for 10 minutes and allowed to cool down. The final volume was adjusted to 5 mL with methanol. The system was equipped with a C_{18} analytical column. The mobile phase was consisted of methanol and water (62:38, v/v). The mobile phase was filtered

through membrane filters and vacuum degassed prior to use. The 10 μL of derivatized solution was injected and eluted isocratically at a flow rate of 1 mL/minute. The UV detector was set at the detection wavelength of 330 nm.

2.2.1.1.2 GABA and OPA+MPA

Method was modified from de Freitas Silva, Ferraz, and Ribeiro (2009), the derivatization was performed by mixing 500 μL of sample or standard solutions, 100 μL of freshly prepared methanolic OPA (25 mg/mL), 375 μL borate buffer (pH 9.9) and 25 μL MPA. The resulting solution was vortexed and analyzed after 1 minute at room temperature. The system was equipped with a C_{18} analytical column. The mobile phase was consisted of 0.05 M sodium acetate, tetrahydrofuran and methanol (50:1:49, v/v) adjusted to pH 4.0. The mobile phase was filtered through membrane filters and vacuum degassed prior to use. Chromatographic analyses was performed at 25 ± 2°C. The 10 μL of derivatized solution was injected and eluted isocratically at a flow rate of 1 mL/min. The fluorescent detector was set at the excitation wavelength of 337 nm and the emission wavelength of 454 nm.

2.2.1.2 Validation for HPLC methods

HPLC analysis methods were validated with typical parameters including specificity, linearity, accuracy and precision (ICH, 2005)

2.2.1.2.1 Specificity

The specificity of HPLC method aimed to ensure that the peak of derivative was free from interference by other components in the sample by comparing the assay results and pure GABA solution.

2.2.1.2.2 Linearity with LOD and LOQ

0.04, 0.06, 0.08, 0.2, 0.4 and 0.6 mg/mL GABA and 0.2, 0.4, 0.5, 0.7 and 0.9 μg/mL GABA were prepared and analyzed for HN and OPA with MPA derivatization, respectively. The relation between peak areas and concentrations were plotted and least square linear regression was calculated. The linearity was determined from the coefficient of determination (R^2). The test was done for three replications. Besides, the low limit of detection (LOD) and the limit of quantitation (LOQ) of GABA under the stated experimental conditions were defined at signal-to-noise (S/N) ratio of 3 and 10, respectively.

2.2.1.2.3 Accuracy

Three concentrations of GABA solution with 0.05, 0.1 and 0.5 mg/mL and 0.3, 0.6 and 0.8 μg/mL for HN and OPA with MPA derivatization, respectively. These concentrations, covering the specified linearity range, were prepared and analyzed (three replicates/concentration). The accuracy was determined from the percentage of recovery.

2.2.1.2.4 Precision

a) Within run precision

Three concentrations of GABA solution with 0.05, 0.1 and 0.5 mg/mL and 0.3, 0.6 and 0.8 μg/mL for HN and OPA with MPA derivatization, respectively. These concentrations, covering the specified linearity range, were prepared and analyzed in the same run (three replicates/concentration). The precision of each concentration was determined from the percentage of coefficient of variation (%CV).

b) Between run precision

Three concentrations of GABA solution with 0.05, 0.1 and 0.5 mg/mL and 0.3, 0.6 and 0.8 μg/mL for HN and OPA with MPA derivatization, respectively. These concentrations, covering the specified linearity range, were prepared and analyzed in three different runs (three replicates/concentration). The precision of each concentration was determined from the percentage of coefficient of variation (%CV).

2.2.1.3 Stability of derivative

GABA derivatives (GABA+HN and GABA+OPA/MPA) were analyzed at different time intervals after derivatization in order to study the stabilities of two studied derivatives. Two derivatizations were sequentially conducted in order to separately monitor the derivative degradations.

2.2.2 Drug loading

Prior to drug loading, the surface of polypropylene microneedles was transformed from hydrophobic to hydrophilic nature by subjecting to an oxygen plasma treatment in a plasma cleaner for 30 minutes. Tips of microneedles were dipped into 5 % GABA aqueous solution and vacuumed for 30 minutes. Then, loaded microneedles were dried in a fume hood overnight. The GABA content was quantified by validated high performance liquid chromatography method. Details were in section 2.2.1.

3. Statistical analysis

Mean and standard deviation were calculated. All experiments were performed at least triplicates. Student's t test was used to analyze the statistical significance between specific pairs of data. Statistically significant difference was shown when the significant level of the test or p value ≤ 0.05.

CHAPTER IV
RESULT AND DISCUSSION

1. Fabrication of polypropylene microneedles

1.1 Preparation of master template

1.1.1 Sewing needle selection

Firstly, sewing needles No. 9 and 11 were selected for the present study. The widths of each needle were measured at the different distances of 0.1, 0.15 and 0.20 mm from the needle tip using an optical microscope to determine the difference of needle size. The means ± SD of three specific widths were compared between needle No. 9 and 11 (Table 1). The results revealed that needle No.9 was bigger than needle No. 11. To select the needle size, the smaller needle No. 11 was chosen to use in the master template because the shape of MNs influenced the skin penetration where small and thin MNs could successfully pierce into the skin (X. Q. Kong, Zhou, and Wu, 2011). Moreover, the smaller tip needle was found to penetrate into the skin more easier than the larger tip needle (Römgens et al., 2014). Thus, the shaper MNs could be produced by the master template made of needle No. 11 and these MNs were more likely to penetrate into the skin successfully.

Table 1 The means of needle widths at three measuring points: 0.10, 0.15 and 0.20 mm from the tip.

Needle size (Number = 140)	**Needle width (Mean ± SD)**		
	At 0.1 mm from the tip	**At 0.15 mm from the tip**	**At 0.20 mm from the tip**
Number 9	68.66 ± 8.20 µm	79.46 ± 8.13 µm	89.80 ± 8.10 µm
Number 11	53.43 ± 6.29 µm	64.74 ± 7.01 µm	75.06 ± 8.41 µm

Other measuring points (i.e., 0.50, 1 and 1.5 mm from the tip) were studied to assure that the selected needles had same or insignificant difference in size or shape. The means ± SD of these specific widths are presented in Table 2. Only needles that have the widths within standard deviation of 10% were selected to produce a master template of MNs.

Table 2 The means of needle widths at three measuring points: 0.50, 1 and 1.5 mm from the tip.

Needle size	**Needle width (Mean ± SD)**		
	At 0.5 mm from the tip	**At 1 mm from the tip**	**At 1.5 mm from the tip**
Number 11 (Before selection) (Number = 125)	108.08 ± 10.16 µm	144.97 ± 6.51 µm	172.69 ± 6.18 µm
Number 11 (After selection) (Number = 42)	109.35 ± 7.01 µm	145.16 ± 4.12 µm	172.78 ± 5.53 µm

1.1.2 Preparation of a microneedle array master template and polypropylene microneedles

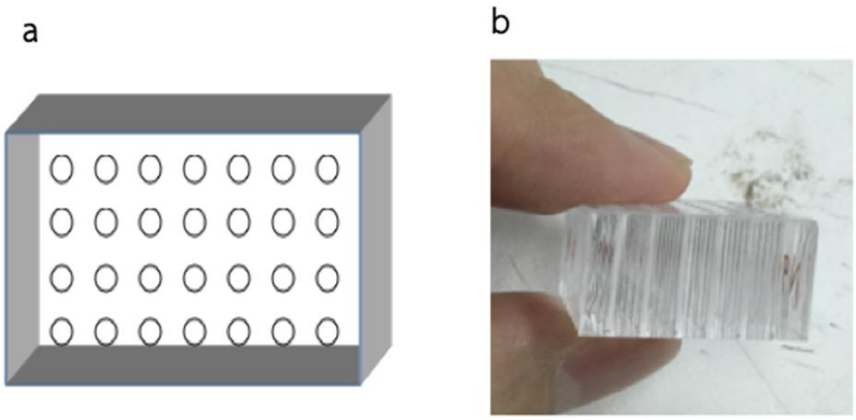

Figure 9 3D Drawing (a) and acrylic master mold box (b)

The master mold box's pattern was designed to have the dimensions of 3 mm in length, 4 mm in width and 5 mm in depth consisting of 42 holes (6x7) with 0.2 mm in radius as shown in Figure 9. Next, the selected needles were inserted into the acrylic box to produce the master template. Later, the obtained master template was glued with epoxy glue and attached to an aluminum plate as in the Figure 10. Polypropylene (PP) was chosen to be used in this study because it is thermo and recycle plastic. It is less expensive and has been used in medical devices (McKeen, 2014; Sastri, 2014). The used PP beads have a melting point of 230 °C according to the certificate of analysis (Polimaxx, Thailand). PP beads were melted by varying the melting temperatures (e.g., 170, 180, 190,…, 240 °C) and holding time (e.g., 10, 15, 20, 25 and 30 minutes) in order to fabricate the MNs with this new fabrication. The optimum melting temperature and holding time were essential for obtaining complete melted PP. The results showed that PP did not melt with the temperature below 200 °C, even if it was held at that temperature for 30 minutes. Higher temperatures (i.e., 210, 220, 230 and 240 °C) and at least 15-minute holding were additionally performed. PP started to change its color to be yellow in less than 15 minutes when heating at 240 °C. Therefore, the melting temperature of 230 °C and 15-minute holding time were chosen to be used in MNs fabrication. At this temperature, the plastic beads could be completely melted with reasonable time and no color change was observed.

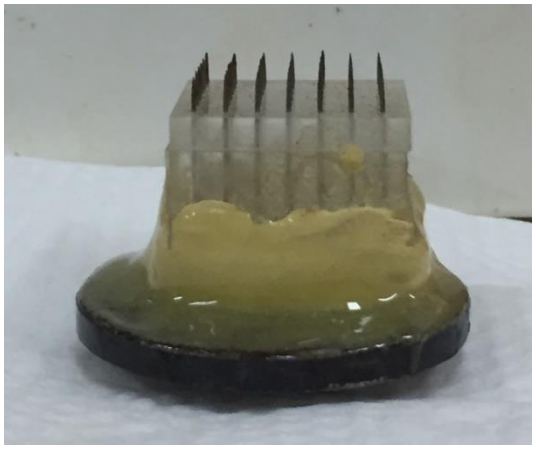

Figure 10 The MNs master template after inserted and glued needles

Later, the plastic MNs was immediately casted after melted PP beads at 230°C and 15 minutes. Unfortunately, the plastic MNs were not successfully casted because the melted plastic was too liquefied and it was difficult to shape up with the lift up master template. The temperature of melted plastic should be lower down to a temperature that the plastic could be easily solidified and shaped up with the lift up master template. After that, several holding temperatures including 170, 180, 190, 200, 210 and 220 °C were studied for 2 hours to find the 2nd temperature which master template could lift off from the molten PP and form the MNs. In summary, the process of casting was divided into two temperature stages with controlled conditions. PP was firstly heated at 230°C for 15 minutes till completely melted. Then, spatula was used to remove excess plastic and make surface plastic smoothen. Secondly, the master template was slowly dipped into melted plastic at predetermined distance (i.e., 1 mm and 1.5 mm) and the system was cooled down to the 2nd temperature for another 2 hours. The master template was lifted up at 1 mm distance to generate plastic MNs, cooled down for 45 minutes, and then the master mold was detached. The results showed that MNs were successfully casted with the 2nd temperature of 180°C for 2 hours. To shorten the process time, higher second temperature (i.e., 180°C) was studied with less holding time of an hour. MNs were successfully casted with the developed conditions. After that, the master template was cleaned with tetrachloroethylene at 60°C modified from (Drain, Murphy, and Otterburn, 1983) and a cutter may be used to remove un-washable plastic from the master mold.

Regarding to this newly developed MNs fabrication process, temperature significantly influenced on the production of plastic MNs. Therefore, the temperature controlled chamber or room may be required for PP MNs fabrication.

2. Characterization of GABA loaded microneedles

2.1 Physical characteristic

2.1.1 Physical appearance of polypropylene microneedles by using SEM and/or optical microscope

Photographs of plastic MNs were taken by digital camera (Figure 11a) and were observed under optical microscope (Figure 11b). SEM image on top view of MNs (Figure 12a) showed the opening drug pocket.

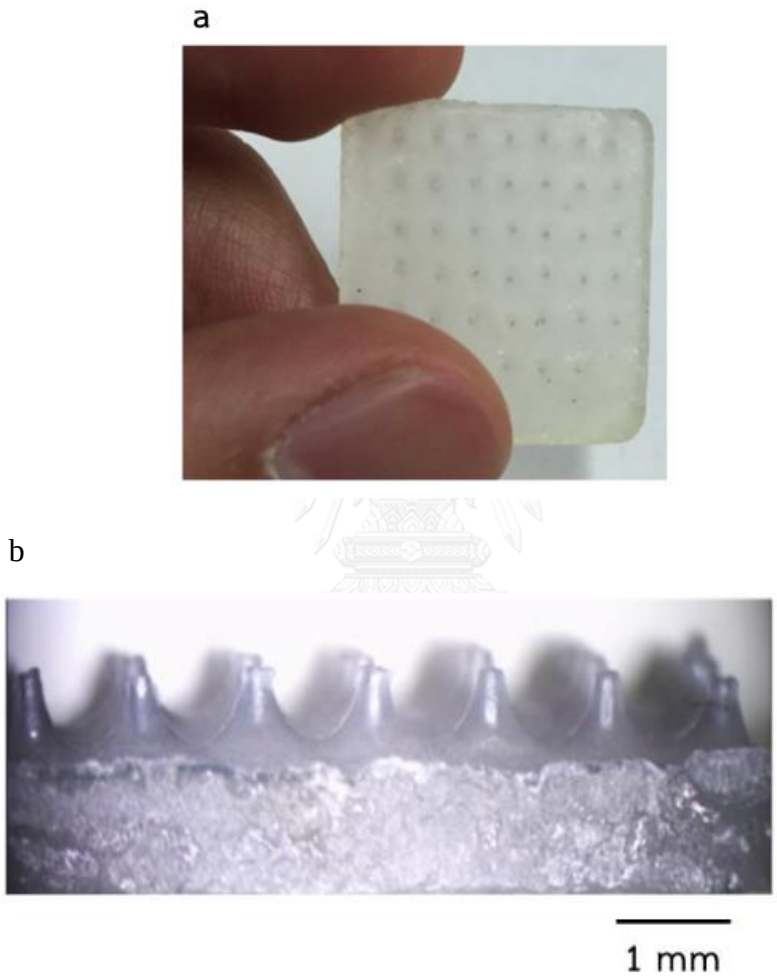

Figure 11 Photographs of MN: (a) normal and (b) under optical microscope

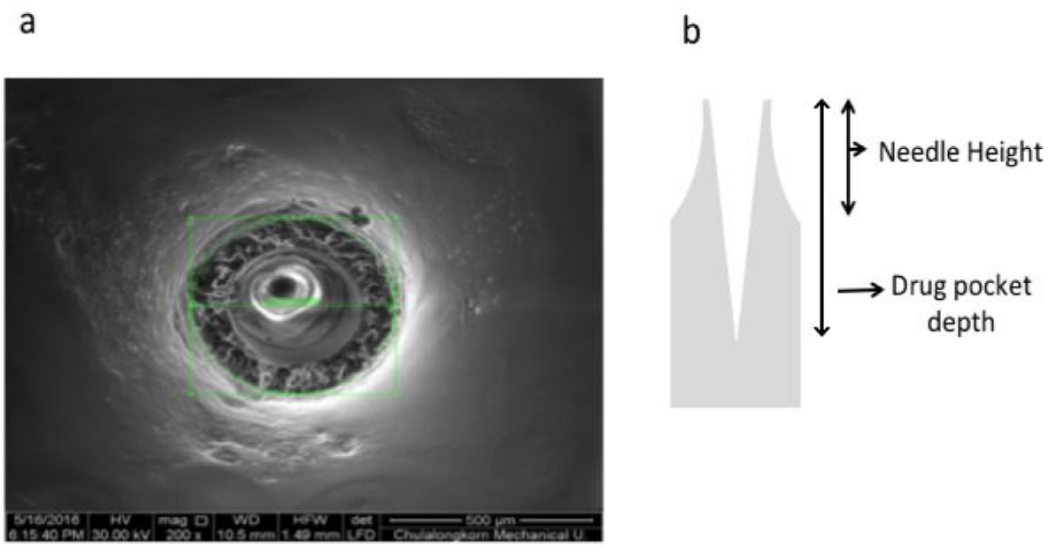

Figure 12 SEM image of MNs (a) and 2D drawing of needle height and drug pocket size (b)

Since the side view of MNs array was clearly observed, those needles (n = 22 per piece) on the four-sides of the MNs array were chosen to measure needle height and drug pocket depth (Figure 12b). The means of needle heights and drug pocket depths of both dipping distances are presented in Table 3 and the data of six MNs arrays are shown. Statistical analysis was performed between the means values of both dipping distances using independent t-test.

One MNs array contains of 42 needles produced by either 1 mm or 1.5 mm dipping distance. With controlled lift up distance, the mean needle heights of two dipping distances were not significantly different at $\alpha = 0.05$ (p-value ≥ 0.05) as shown in Table 3. Needle height could be controlled by fixing lift up distance (1 mm) but different drug pocket sizes could be varied by dipping distance. The results revealed that the mean pocket depths of two dipping distances were significantly different at $\alpha = 0.05$ (p-value < 0.05) as shown in Table 3. The drug pocket size could be easily varied by dipping distance and could result in different drug loading capacities.

Table 3 The means of needle heights and drug pocket depths of plastic MNs with two dipping distances

Microneedles array No. (n=22/piece)	**Needle height (Mean ± SD in mm)**		**Drug pocket depth (Mean ± SD in mm)**	
	Dipping distance 1 mm	**Dipping distance 1.5 mm**	**Dipping distance 1 mm**	**Dipping distance 1.5 mm**
1	1.06 ± 0.12	0.96 ± 0.17	0.98 ± 0.05	1.44 ± 0.12
2	1.01 ± 0.12	0.98 ± 0.12	0.94 ± 0.08	1.45 ± 0.07
3	1.12 ± 0.20	1.03 ± 0.15	0.98 ± 0.12	1.44 ± 0.07
4	0.97 ± 0.16	1.02 ± 0.12	0.93 ± 0.10	1.48 ± 0.08
5	1.01 ± 0.13	1.05 ± 0.14	0.99 ± 0.08	1.47 ± 0.07
6	1.00 ± 0.16	1.03 ± 0.17	0.94 ± 0.1	1.47 ± 0.09
Average	**1.03 ± 0.15**	**1.01 ± 0.15**	**0.96 ± 0.09**	**1.46 ± 0.09***

* statistical difference between two dipping distances ($p<0.05$)

Moreover, the outer and inner radiuses of the opening drug pocket were measured for both dipping distances (Table 4). Thirteen needles were randomly selected and performed the measurements for each MNs array and total of six arrays were measured With this number of sample size, the power of the test was 94.84 % and 95.40 % for 1 mm and 1.5 mm dipping distance, respectively ($\alpha = 0.05$, $\delta = 20$ µm and $\sigma_{\text{inner radius}}$). Sigma ($\sigma$) was obtained from the measurement of inner radius because it was used to calculate volume of drug loading. Statistical analysis was performed between the means values of both dipping distances using independent t-test.

The needles used in MNs arrays were selected as previously mentioned; therefore, MNs produced by two dipping distances showed similar inner radius with insignificant difference ($p>0.05$) as shown in Table 4. While there was significant difference between outer radiuses of MNs made from two dipping distances as shown in Table 4. This new fabrication process allowed the melted thermoplastic to cool down and set without any extra drying process. This uncontrolled drying environment could influence on outer radius more than inner radius of produced MNs. Controlled

drying environment is recommended for further development. Moreover, inner radiuses were not correlated with the reported needle widths at two reference points (i.e., 1 mm or 1.5 mm) (Table 2). This may be due to the fact that setting process of this thermoplastic under this fabrication conditions is not fully understood.

Table 4 The means of outer and inner radiuses of drug pocket with two dipping distances

Microneedles array No. (n=13/piece)	**Outter radius (Mean ± SD in μm)**		**Inner radius (Mean ± SD in μm)**	
	Dipping distance 1 mm	**Dipping distance 1.5 mm**	**Dipping distance 1 mm**	**Dipping distance 1.5 mm**
1	254.16 ± 117.80	231.8 ± 24.55	155.13 ± 11.62	160.79 ± 9.93
2	244.59 ± 19.50	231.28 ± 22.79	171.45 ± 18.68	164.53 ± 12.15
3	236.79 ± 15.43	217.11 ± 27.76	157.72 ± 12.25	151.53 ± 8.84
4	280.52 ± 18.81	242.33 ± 32.08	159.85 ± 11.55	160.07 ± 12.39
5	251.2 ± 21.70	246.85 ± 24.27	152.13 ± 11.34	172.83 ± 13.01
6	246.03 ± 14.05	231.71 ± 20.64	155.6 ± 9.37	160.65 ± 19.09
Average	**253.74 ± 21.73**	**233.51 ± 26.36***	**158.07 ± 14.19**	**161.73 ± 13.98**

* statistical difference between two dipping distances ($p<0.05$)

2.1.2 Failure strength test

Failure strength test could not perform with whole MNs array due to insufficient applied force. Therefore, MNs array was cut into a small portion of four needles per piece. The relationship between applied force pre needle and displacement of each sample (n=6) is presented in Figure 13 along with 95% confidence interval of mean. Figure 13a shows the data of MNs made from 1.0 mm dipping distance and Figure 13b shows the data of MNs made from 1.5 mm dipping distance.

a

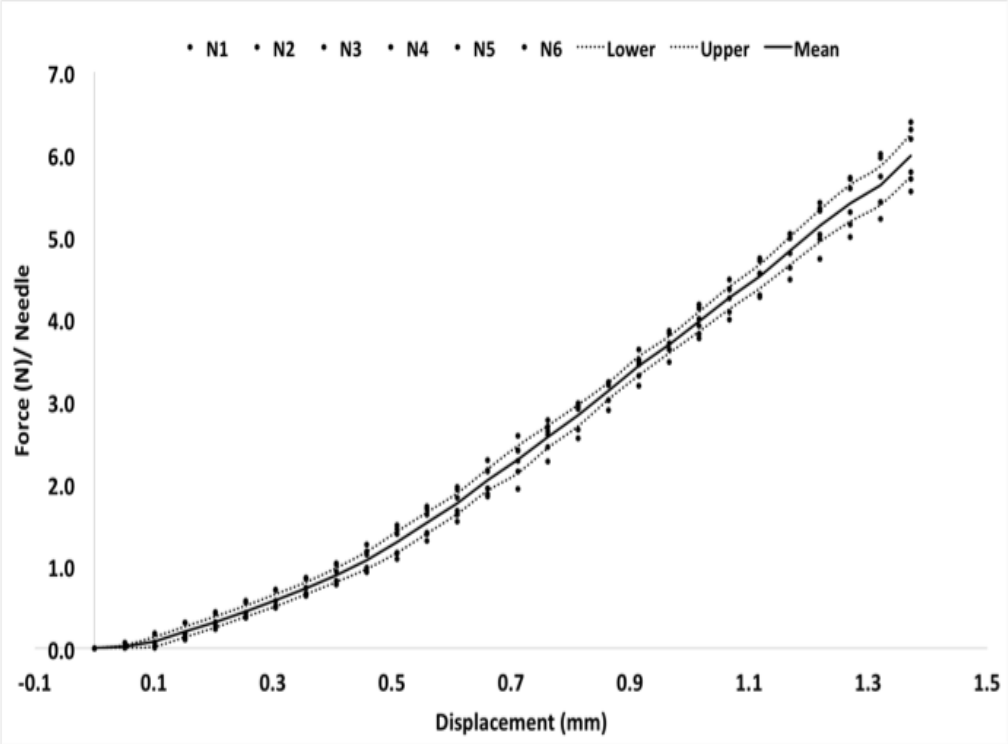

b

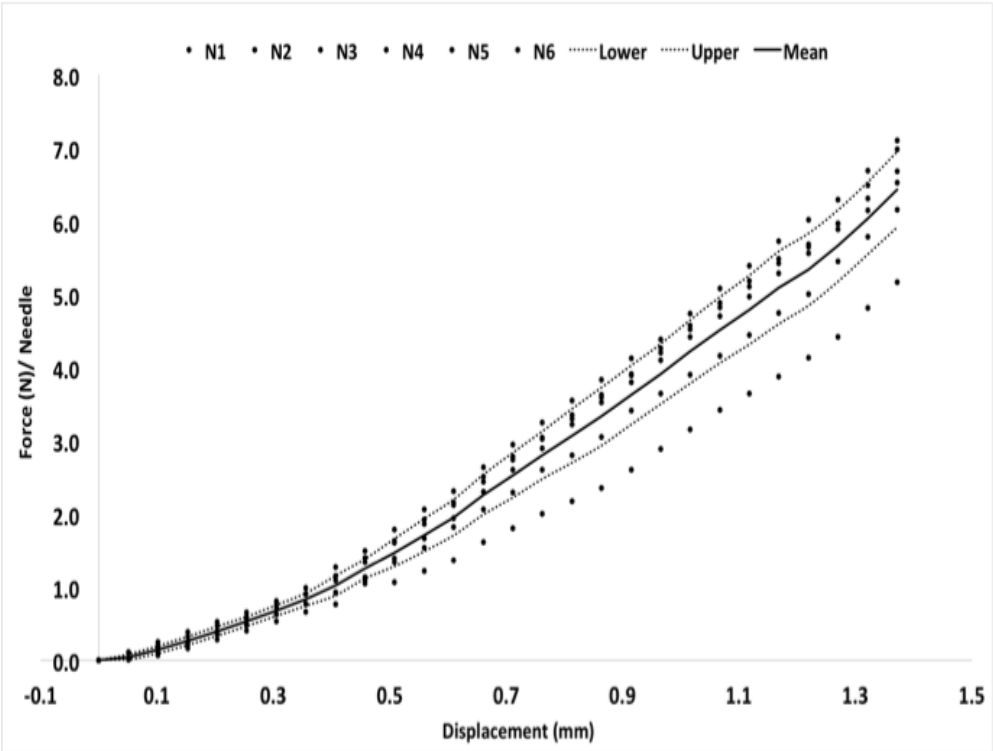

Figure 13 Failure strength tests of MNs made from 1 mm (a) and 1.5 mm (b) dipping distance

a

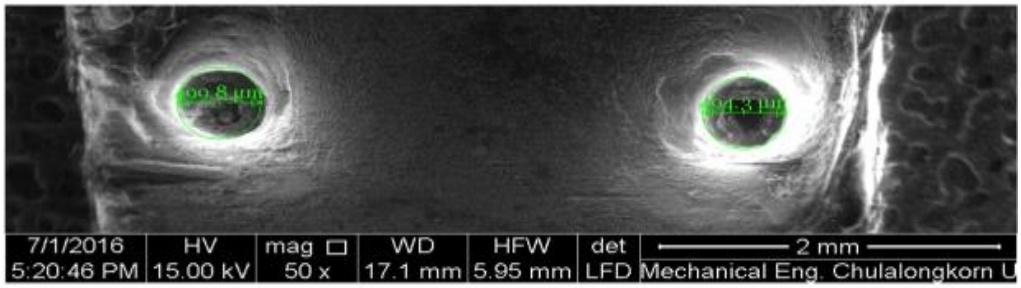

b

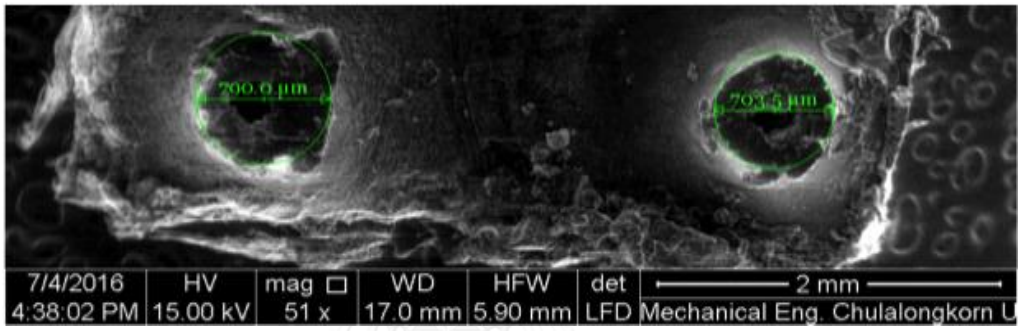

Figure 14 SEM images of MNs after failure strength test: MNs made from 1 mm (a) and 1.5 mm (b) dipping distance.

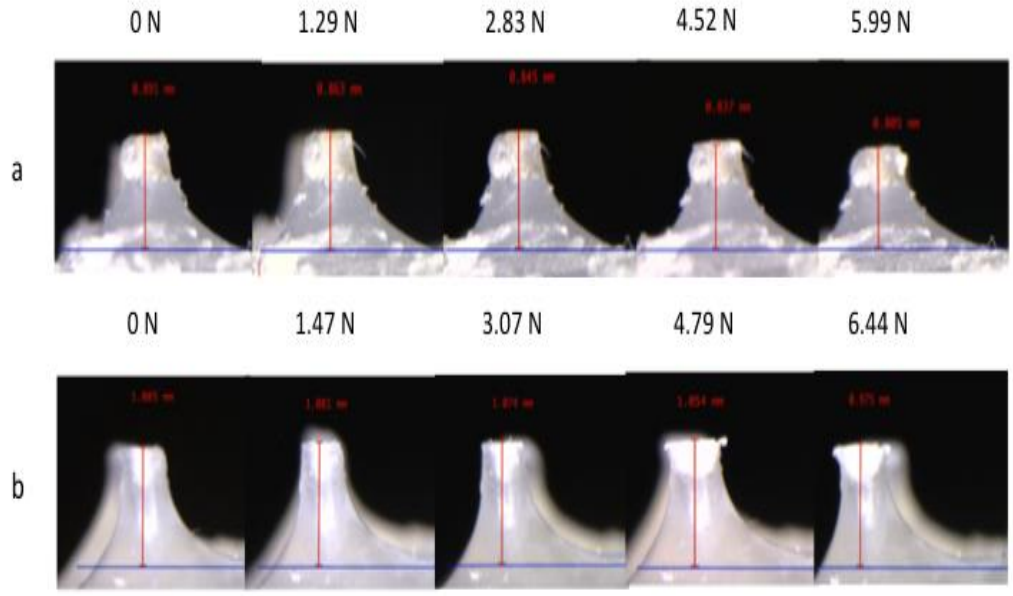

Figure 15 Microscopic side views of MNs before the failure strength test after applied force: MNs made from 1 mm (a) and 1.5 mm (b) dipping distance

SEM images were taken after the test where Figure 14a-b show the top views of the needles cast from 1 mm and 1.5 mm dipping distance, respectively. The side views of MNs were photographed under microscope at different time intervals including before the test or 0 sec and 50 sec, 85 sec, 115 sec and 150 sec after happlied applied force as shown in Figure 15a (1 mm dipping distance) and Figure 15b (1.5 mm dipping distance).

Failure strength test plots (Figure 13a-b) show linear relationship between applied force and displacement but a maximum fraction force point did not appear. On the other hand, both MNs could withstand applied force (6 N/needle) without significant deformation or fracture. This may be because MNs was made of plastic. All test samples in each dipping distance showed similar failure strength test curves except one sample of 1.5 mm dipping distance. Because this MNs fabrication was primitive work and the test samples were randomly selected so the selected needles could be smaller or shorter than other samples. Shorter needle would expect to withstand more applied force because it would take some distance before the stage pressed onto the needle. SEM image and microscopic images also agreed with the failure strength test that there was no significant deformation or fracture but only slight unsharpened needle tip was observed (Figure 14a-b and 15a-b). As previously mentioned, with fixed lift up distance, same needle height was obtained for both dipping distances. Consequently, both MNs should withstand the same applied force without fracture. Outer radiuses of both MNs were significantly increased with $p<0.05$ (Table 5).

Plastic property is very important factor for molded plastic. Among many factor, the compressive yield strength is one that can influence the fracture force of molded plastic. The compressive yield strength is a factor that shows the strength of material against the hard surface like stainless steel or aluminum, which larger number represents more powerful material strength. The compressive yield strength of PP found to be 40 MPa which implied that PP has quite strong property (MatWeb, n.d.). In addition, the shape of the MNs was also known to have an effect on the fraction force. This new special design MNs had wider tip which could result in stronger needle when pressing against harder surface compared with sharper MNs (Bystrova and Luttge, 2011).

Table 5 The mean of the outer radius of drug pockets with two dipping distances before and after the failure strength test

Microneedles array No. (n=4/piece)	**Outer radius (Mean ± SD in µm)**			
	Dipping distance 1 mm		**Dipping distance 1.5 mm**	
	Before	**After**	**Before**	**After**
1	321.64 ± 19.07	300.26 ± 18.69	266.71 ± 14.71	302.76 ± 33.46
2	370.09 ± 15.78	394.61 ± 35.19	224.71 ± 12.89	262.89 ± 29.85
3	279.63 ± 47.34	307.98 ± 68.76	258.49 ± 21.78	337.35 ± 65.77
4	232.13 ± 18.79	310.78 ± 59.72	261.6 ± 15.55	328.65 ± 31.75
5	233.54 ± 18.82	306.73 ± 68.06	274.31 ± 5.99	345.25 ± 49.53
6	256.90 ± 22.44	306.19 ± 81.36	253.41 ± 22.50	309.09 ± 63.06
Average	**282.32 ± 54.41**	**321.09 ± 36.18 ***	**256.54 ± 17.16**	**314.33 ± 29.99****

* statistical difference between before and after the failure strength test for 1 mm dipping distance ($p<0.05$)

** statistical difference before and after the failure strength test for 1.5 mm dipping distance ($p<0.05$)

2.1.2 Skin penetration test

Skin penetration study was conducted on excised pig dorsal skin. Full thickness pig dorsal skin was obtained from newborn pig which naturally died and was stored under -20 °C till time to use. The standard weight of 3, 5 or 7 kg was pressed onto MNs which were placed on top of mounted pig skin for 30 seconds. The maximum of 7 kg standard weight was chosen because the additional weight could not be positioned directly onto the MNs without shaking. Stained microtome pig skin after the penetration test is presented in Figure 16.

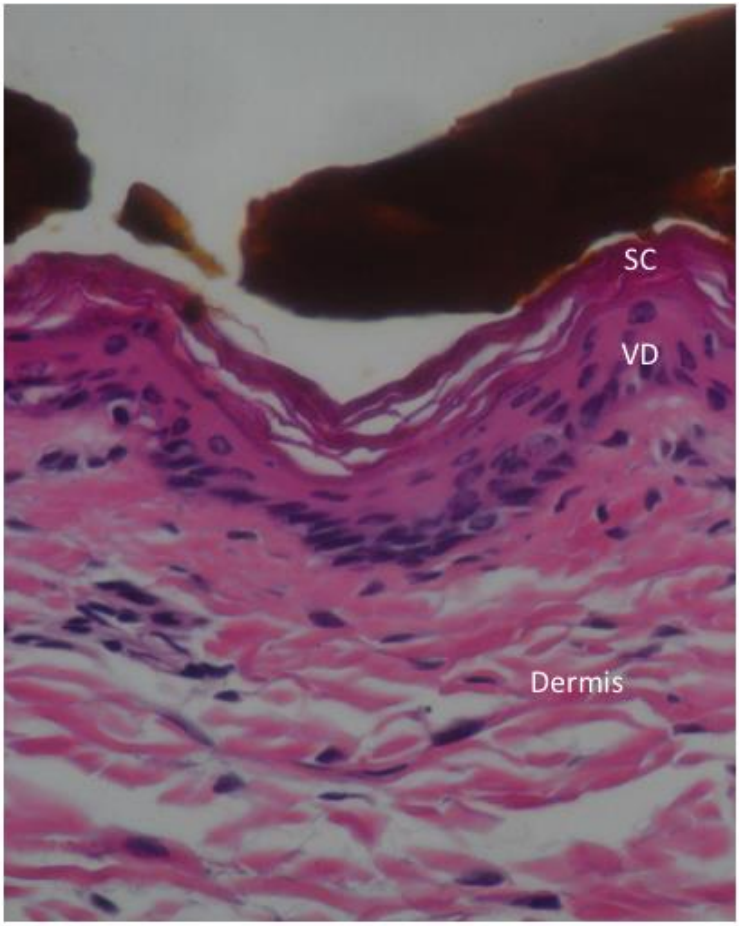

Figure 16 Stained microtome pig skin after the penetration test (SC: stratum corneum, VE: viable epidermis) using an optical microscope

Henry et al. (1998) proposed the theoretical insertion pressure to pierce the skin of 3.183 x 10^6 Pa (N/m^2) per needle which was linearly dependent on the surface area of the tip. The metal MNs with sharp tips (radius less than 1 μm) and 150 μm in height was used for this estimation. The predicted force to pierce the skin for each MNs type was calculated according to this equation (3.183 x 10^6 x surface area). The forces were 0.64 N or 0.065 kg/needle/m^2 and 0.54 N or 0.055 kg/needle/m^2 for dipping size 1 mm and dipping size 1.5 mm, respectively. The use of the maximum force 7 kg/30 sec was expected to successfully insert MNs into the skin. Unfortunately, this force unsuccessfully inserted MNs into the pig skin as shown in Figure 16. The result revealed the predicted force from the equation was not relevant to be used with this newly developed MNs. Several reasons could explain these results including the material type used to develop the equation was metal which is

stronger than the plastic and the shape of the metal MNs was shape but these studied MNs had a hole in center of wider needle tip which may require more force than the predicted force to insert the skin.

Different needle tip shapes have different tip surfaces which appeared to require different insertion forces (X. Q. Kong, Zhou, and Wu, 2011; Römgens et al., 2014). Henry et al. (1998) reported that the tip surface was linearly correlated with the insertion force which also found in the study of Puneet et al. (2010) about silicon hollow MNs with cylindrical shape and 120 μm height. Hollow MNs with 80 μm outer tip radius and 42.5 μm inner tip radius (14,431 μm^2 tip area) needed insertion force (≥ 7.5 N/piece) more than hollow MNs with 76.95 μm outer tip radius and 48.9 μm inner tip radius (11,083 μm^2 tip area) which the insertion force was about 4.75 N/piece. They mentioned that the large surface area needed more insertion force than the smaller in skin penetration. Thereby, etching of master template's needles is one way to thin down the needle tip and make more shaper needle which should successfully insert MNs into the skin with lower insertion force.

Very first prototype of this new MNs fabrication had unequal needle heights which may cause the given force less effective to penetrate the skin. Cutting MNs tip in the last step of fabrication (such as 1 mm or less) may make MNs equal in height. Process parameters of MNs fabrication should be further refined in order to produce more precise size of MNs such as control precisely temperature in fabrication process. Moreover, application of applicator may be used to facilitate the insertion of MNs as evidenced by Verbaan et al. (2008). Another research, fused-silica hollow MNs with 187.5 μm outer tip radius and 10 μm inner tip radius also used an applicator to improve skin penetration. The applied velocity of 1 m/s could help the MNs' penetration to about 110 μm depth into the skin (van der Maaden et al., 2014).

More sharpen needle tip and optimum needle height should be further developed to successfully penetrate the skin deep enough to cross the stratum corneum barrier but not should so deep to hit nerves and cause pain.

2.2 Chemical characterization

2.2.1 Drug content by GABA analysis by High performance liquid chromatographic (HPLC) method

In comparison, the preparation of GABA+HN derivative required heating at 80 °C and time to form whereas the preparation of GABA+OPA/MPA derivative did not require energy and the derivative was formed in a minute. Both derivatives were successfully prepared.

2.2.1.2 HPLC method validation

2.2.1.2.1 Specificity

To confirm an ability of the HPLC analysis to separate the interested substance from the other compounds with no interfere is called the specificity. The HPLC chromatograms of buffer, standard GABA solution and derivatizing agent before and after derivatization with HN and OPA/MPA were presented in Figure 17 and Figure 18, respectively. The retention time of GABA + HN derivative was about 3 min and the run time was within 15 min per injection. Whereas the retention time of GABA + OPA with MPA derivative was about 5 min and the run time was within 10 min per injection. All chromatograms are presented under the same attenuation and scale. The results showed that derivatives' peaks were free of interference and were clearly separated from their derivatizing agent. Therefore, the two HPLC methods were acceptable for the specificity.

2.2.1.2.2 Linearity

In order to quantify GABA in the sample, standard calibration curve was generated in the optimum concentration range. The calibration curves of HN and OPA/MPA derivatizations are presented in Figure 18a and Figure 18b, respectively. Linear correlation was obtained between peak areas and concentrations of GABA + HN and GABA + OPA/MPA in the range of 0.04-0.6 mg/mL ($r^2 > 0.999$) and 0.2-0.9 μg/mL ($r^2 > 0.998$), respectively. These results indicated that both methods were acceptable to quantify GABA in the studied ranges.

2.2.1.2.3 LOD and LOQ

The LOD is the lowest concentration of the sample that can be detected (but not necessarily to be quantitated) under the stated experimental conditions. The LOQ is the lowest concentration in a sample that may be measured with an acceptable level of accuracy and precision. The LOD and LOQ for GABA+HN derivative were found 0.001 mg/mL and 0.005 mg/mL, respectively. Where, the LOD and LOQ for GABA+OPA/MPA derivative were much lower (i.e., 0.004 μg/mL and 0.02 μg/mL, respectively). More sensitive method could be attained with OPA/MPA derivatization when compared with HN regarding to significantly lower concentration detected.

2.2.1.2.4 Precision

The precision of an analytical method expresses the closeness of agreement between series of measurements gained from multiple sampling of the same homogeneous sample under the condition. The precision assesses using 3 concentration levels covering the specified range.

Three concentrations of 0.05, 0.1 and 0.5 mg/mL for GABA+HN and 0.3, 0.6 and 0.8 μg/mL for GABA+OPA/MPA were chosen for both precision and accuracy studies. Both within run and between run were preformed for precision study, which are presented in Table 6-7 for GABA+HN and Table 8-9 for GABA+OPA/MPA. Both CV values for precision were good (<6% CV) which could reveal that both methods were reproducible in the studied range.

2.2.1.2.5 Accuracy

The accuracy of an analytical method expresses the closeness of agreement between the value which is accepted for a conventional true value or an accepted reference value and the value found. The accuracy assesses using 3 concentration levels covering the specified range.

The percentages of analytical recovery were close to 100% and are presented in Table 10-11. These results informed that HPLC analysis using these two derivatizing agents were accurate on quantitation of GABA.

2.2.1.3 Stability of two derivatives

Since two derivatives were unstable and could degrade, the stability studies were conducted to determine the length of time that the derivative could be kept before analysis without significant degradation.

GABA concentrations were monitored over time intervals and the plots of GABA concentration remained versus time after the derivatization for both derivatizing agents are shown in Figure 19. The results revealed more than about 99 % of GABA+HN derivative remained over 4 hours after the derivatization whereas GABA+OPA/MPA derivative was fallen below 80 % (slope = - 0.3039) in less than an hour. In comparison, more stable derivative could be obtained with HN derivatizing agent. In addition, analysis of GABA using HN would be less time constrained.

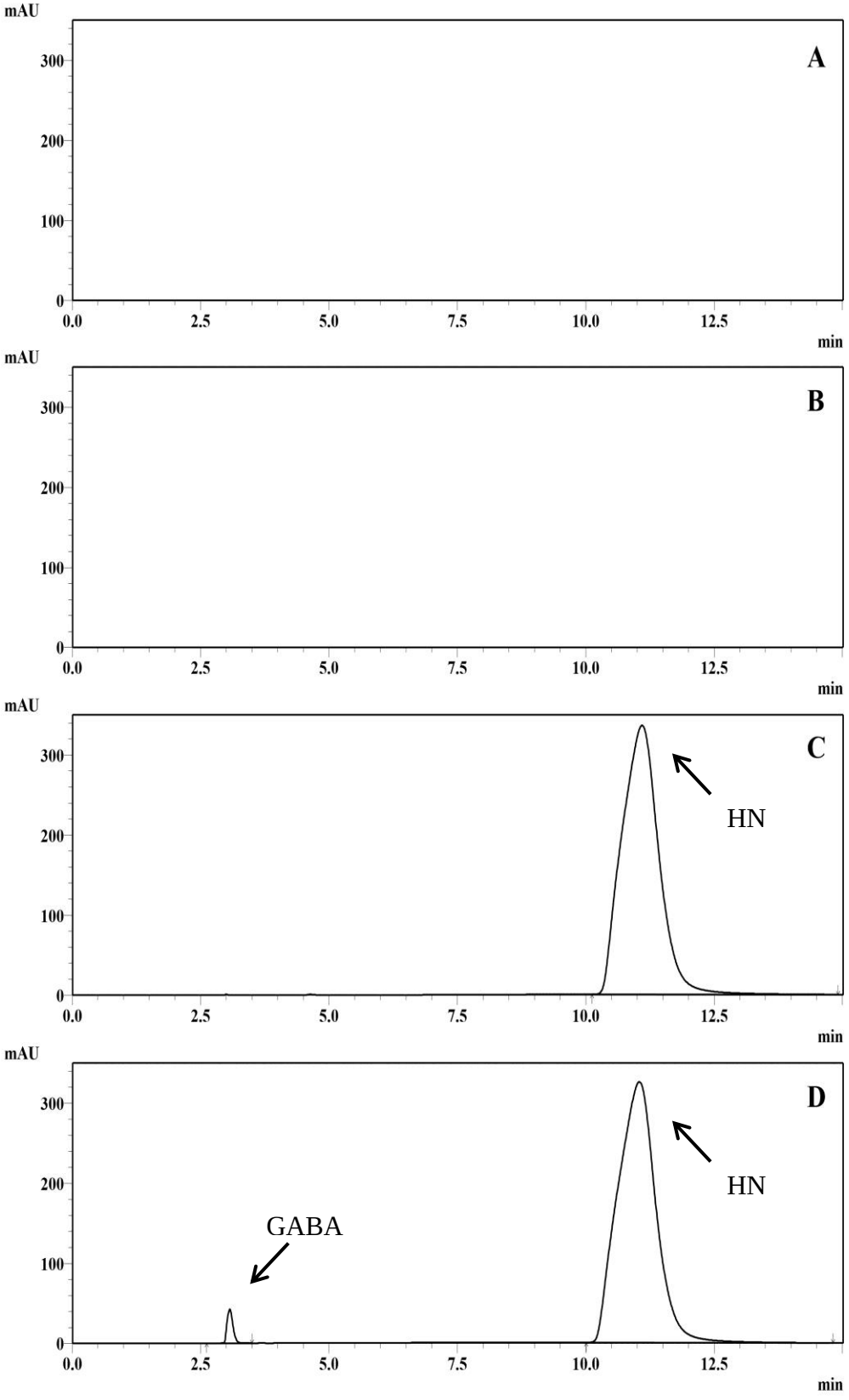

Figure 17 HPLC-UVD chromatograms of a) buffer system b) 0.8 mg/mL GABA c) HN and d) 0.04 mg/mL GABA+HN

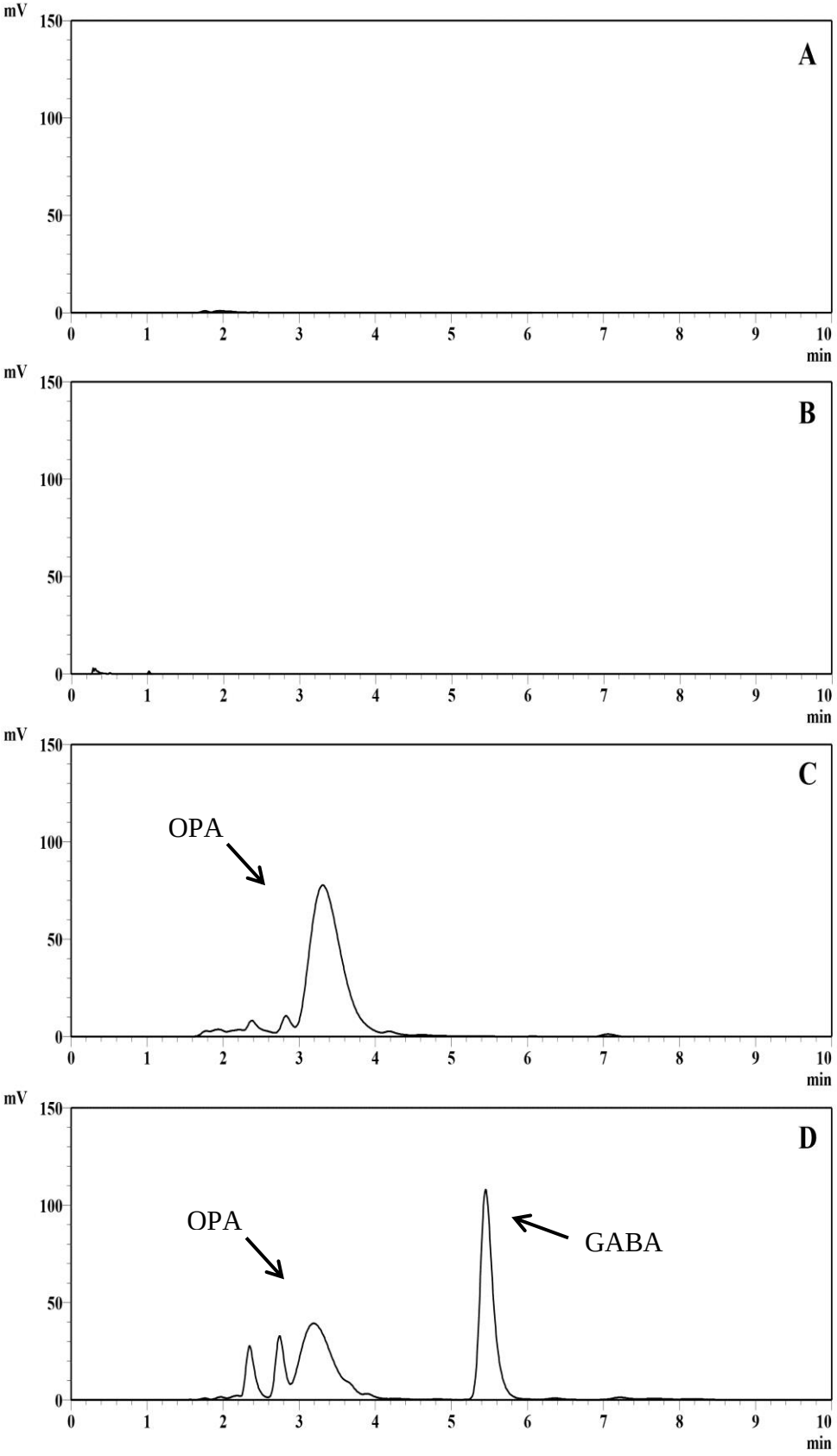

Figure 18 HPLC-FD chromatograms of a) buffer system b) 1 μg/mL GABA c) OPA+MPA and d) 0.1 μg/mL GABA+OPA/MPA

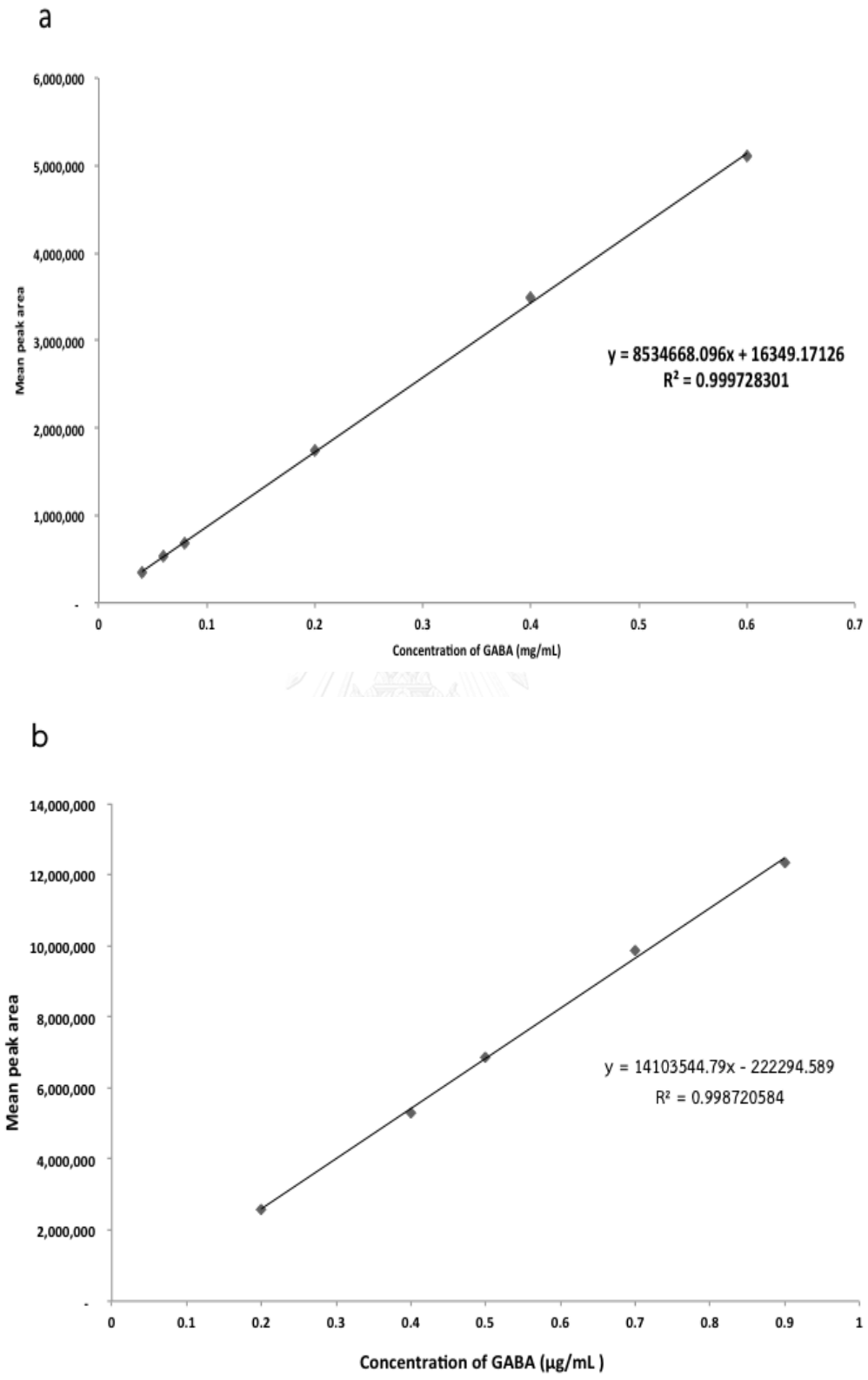

Figure 19 The calibration curves of (a) GABA+HN and (b) GABA+OPA with

Table 6 Intra-day precision (%CV) of GABA+HN derivative by HPLC-DAD method

Concentration (mg/mL)	Inversely estimated concentration (mg/mL)			Mean	SD	CV
	Set 1	Set 2	Set 3			
0.5	0.4712	0.4822	0.4805	0.4780	0.0048	1.0115
0.1	0.0982	0.0967	0.0943	0.0943	0.0016	1.6662
0.05	0.0489	0.0475	0.0500	0.0488	0.0010	2.0964

Table 7 Inter-day precision (%CV) of GABA+HN derivative by HPLC-DAD method

Concentration (mg/mL)	Inversely estimated concentration (mg/mL)			Mean	SD	CV
	Set 1	Set 2	Set 3			
0.5	0.4690	0.5122	0.5276	0.5029	0.0248	4.932
0.1	0.1010	0.1018	0.1054	0.1027	0.0019	1.8628
0.05	0.0485	0.0485	0.0499	0.0490	0.0007	1.3478

Table 8 Intra-day precision (%CV) of GABA+OPA with MPA derivative by HPLC-FD method

Concentration (μg/mL)	Inversely estimated concentration (μg/mL)			Mean	SD	CV
	Set 1	Set 2	Set 3			
0.8	0.9110	0.9138	0.8996	0.9081	0.0061	0.6763
0.6	0.6217	0.6354	0.6167	0.6246	0.0076	1.2656
0.3	0.3205	0.3427	0.3304	0.3312	0.0091	2.7418

Table 9 Inter-day precision (%CV) of GABA+OPA with MPA derivative by HPLC-FD method

Concentration (μg/mL)	Inversely estimated concentration (μg/mL)			Mean	SD	CV
	Set 1	Set 2	Set 3			
0.8	0.8311	0.7749	0.8349	0.8136	0.0274	3.3716
0.6	0.6180	0.5669	0.6370	0.6073	0.0296	4.8743
0.3	0.3087	0.2713	0.2826	0.2875	0.0157	5.4470

Table 10 Accuracy (%recovery) of GABA+HN derivative by HPLC-DAD method

Concentration (mg/mL)	% Analytical recovery			Mean ± SD
	Set 1	Set 2	Set 3	
0.5	102.78	99.46	99.81	100.68 ± 1.49
0.1	104.41	102.07	101.97	102.82 ± 1.13
0.05	92.04	101.42	99.47	97.64 ± 4.04

Table 11 Accuracy (%recovery) of GABA+OPA with MPA derivative by HPLC-FD method

Concentration (μg/mL)	% Analytical recovery			Mean ± SD
	Set 1	Set 2	Set 3	
0.8	99.46	102.27	103.45	101.73 ± 1.67
0.6	98.09	100.91	104.74	101.25 ± 2.73
0.3	95.93	101.12	90.58	95.88 ± 4.30

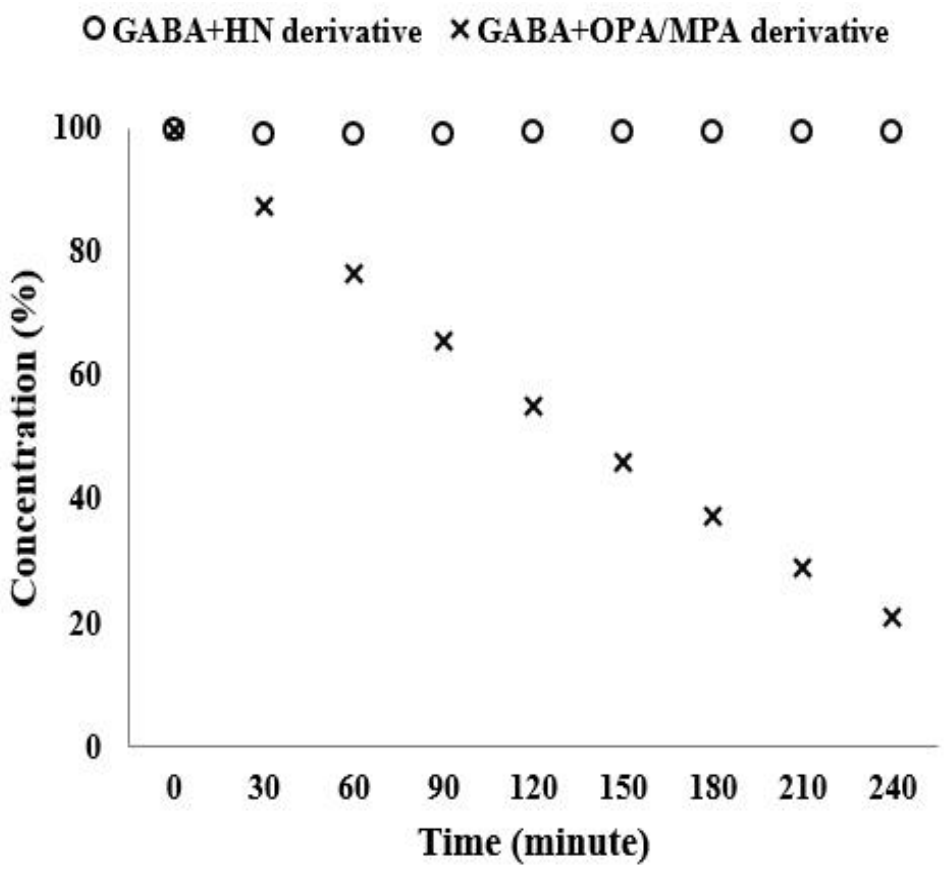

Figure 20 Stability profiles of GABA+HN and GABA+OPA with MPA derivatives

2.2.2 Drug loading

Water soluble dye, methylene blue, was initially used instead of GABA to optimize process parameters (because it is clearly seen with its stain). In the first step, MNs were treated by plasma cleaner for 30 minutes in order to increase the hydrophilic property on MNs' surface. Next, the MNs were loaded with methylene blue by capillary force with aid of vacuum oven. Methylene blue loaded pockets were clearly observed as shown in Figure 21. Moreover, the durations of vacuum oven for drug loading were varied (e.g., 10, 20 and 30 minutes). Thirty minutes of vacuum oven showed the most dye loading by observing the color density. Thereby, MNs were treated with plasma cleanser for 30 minutes and following by drug loading under vacuum oven for 30 minutes. Last, 5 % GABA was loaded into two types of MNs (six patches per each type). Next, loaded MNs were dried at room temperature overnight.

After MNs were completely prepared, loaded MNs were analyzed for GABA content. Loaded MNs were dipped in known volume of DI water and sonicated for 30 minutes to ensure that complete dissolution of GABA was achieved. Resulted solution was quantified for GABA. Since OPA/MPA derivatization were more sensitive method, this method was chosen for drug loading study. GABA quantities of both MNs types are presented in Table 12. Theoretical loading volume was calculated by inner radius of each dipping distance and summed up to the volume per piece. Then, the volume was converted to theoretical drug loading or drug content (μg/piece) for these MNs. The HPLC analytical results showed that the recovery drug amount of two MNs were higher than the predicted values about 10 times for dipping distance 1 mm and about 8.3 times for dipping distance 1.5 mm because the recovery drug content included the drug coated outside the pocket of MNs due to the way of loading process. However, outside geometry and appearance of MNs were assumed to be similar because the two types were made of the same master template and same tray. Thus, the amount of drug coated should be not significantly different from each other. When comparing the ratio of pocket depths for two MNs types, the theoretical value should be 1.5. However, the ratio of drug loadings between two dipping distances was only about 1.3. MNs with dipping distance 1.5 mm had deeper drug pocket compared with the one with 1 mm dipping distance so the air bubble may be trapped in the bottom of drug pocket and prevented the drug to be completely loaded. As a result, the recovery drug ratio between two MNs showed relative lower than theoretically calculated.

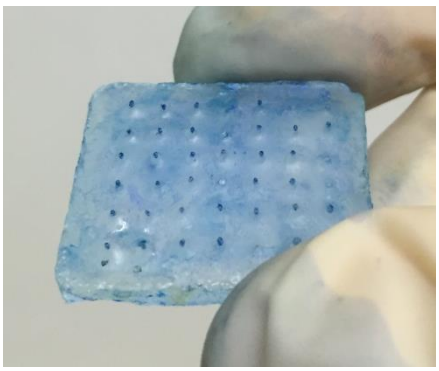

Figure 21 Methylene blue loaded MNs pocket

Table 12 GABA loadings of MNs made from two dipping distances

MNs (piece)	Theoretical volume loading (µL/piece)		Theoretical drug loading (µg/piece)		Found drug loading (µg/piece)	
	Dipping distance 1 mm	**Dipping distance 1.5 mm**	**Dipping distance 1 mm**	**Dipping distance 1.5 mm**	**Dipping distance 1 mm**	**Dipping distance 1.5 mm**
1	1.06	1.71	53.00	85.50	561.00	723.00
2	1.29	1.79	64.50	89.50	462.00	649.50
3	1.09	1.51	54.50	75.50	760.50	723.00
4	1.12	1.69	56.00	84.50	477.00	838.50
5	1.02	1.97	51.00	98.50	454.50	709.50
6	1.06	1.70	53.00	85.00	592.50	648.00
Average	**1.07**	**1.72**	**53.50**	**86.00**	**551.25**	**715.25***

* significant difference between two dipping distances ($p<0.05$)

MNs made of 1.5 mm dipping distance showed more drug loading as a result of larger drug pocket produced from deeper dipping distance when compared with 1 mm dipping distance at p-value less than 0.05. This new MNs with auto-generated drug pocket could be tailor-made the drug pocket size by varying the dipping distance. As a consequence, this innovative MNs could be used to deliver a small and water-soluble molecule like GABA and can be loaded with various drug quantities.

CHAPTER V
CONCLUSIONS

Water soluble molecules, which the targeting site of action is underneath stratum corneum (SC), may have problems with skin permeation to get into the target site by themselves. There are many ways to improve those molecules going through the SC. Microneedles patch is one of the promising methods which has been proved that could successfully bypass the skin barrier. Application of MNs to deliver the interested molecule, GABA, was explored in this current study. Newly invented MNs fabrication of PP was developed in terms of process parameters and parameter which could affect the auto-generated drug pocket i.e., dipping distance. PP MNs were casted with two dipping distances (1 mm and 1.5 mm). PP MNs were successfully produced from different dipping distances and showed different capacities of GABA loading because of different pocket sizes. Unfortunately, the new MNs could not penetrate the SC even using press force at 7 kg/patch. Further development of this novel MNs is needed to be able to break into the skin. However, this primitive prototype of PP MNs with newly invented fabrication method showed promising early results to be a potential delivery system of small and water soluble molecule through the skin.

REFERENCES

Abdou, A. M., Higashiguchi, S., Horie, K., Kim, M., Hatta, H., & Yokogoshi, H. (2006). Relaxation and immunity enhancement effects of γ-aminobutyric acid (GABA) administration in humans. Biofactors, *26*(3), 201-208.

Agache, P. G., Agache, P., & Humbert, P. (2004). *Measuring the skin*: Springer Science & Business Media.

Aktan, F. (2004). iNOS-mediated nitric oxide production and its regulation. Life Sciences, *75*(6), 639-653.

Amihăesei, I., & Mungiu, O. (2011). Main neuroendocrine features and therapy in primary sleep troubles. Revista medico-chirurgicala a Societatii de Medici si Naturalisti din Iasi, *116*(3), 862-866.

Anderson, R. R., & Parrish, J. A. (1982). Optical properties of human skin. In J. D. Regan and J. A. Parrish (Eds.), *The Science of Photomedicine* (pp. 147-194). Boston, MA: Springer US.

Andrae, J., Gallini, R., & Betsholtz, C. (2008). Role of platelet-derived growth factors in physiology and medicine. Genes & Development, *22*(10), 1276-1312.

Archer, C. B. (2010). Functions of the skin *Rook's Textbook of Dermatology* (pp. 1-11): Wiley-Blackwell.

Awapara, J., Landua, A. J., Fuerst, R., & Seale, B. (1950). Free γ-aminobutyric acid in brain. Journal of Biological Chemistry, *187*, 35-39.

Barbero, A. M., & Frasch, H. F. (2009). Pig and guinea pig skin as surrogates for human in vitro penetration studies: A quantitative review. Toxicology in Vitro, *23*(1), 1-13.

Bouwstra, J. A., Groenink, H. W. W., Kempenaar, J. A., Romeijn, S. G., & Ponec, M. (2008). Water distribution and natural moisturizer factor content in human skin equivalents are regulated by environmental relative humidity. Journal of Investigative Dermatology, *128*(2), 378-388.

Brenes, R. A., Ajemian, M. S., Macaron, S. H., Panait, L., & Dudrick, S. J. (2011). Initial experience using a hyaluronate-iodine complex for wound healing. The American Surgeon, *77*(3), 355-359.

Brown , G. L., Nanney , L. B., Griffen , J., Cramer , A. B., Yancey , J. M., Curtsinger , L. J. I., . . . Lynch , J. B. (1989). Enhancement of wound healing by topical treatment with epidermal growth factor. New England Journal of Medicine, *321*(2), 76-79.

Bruch-Gerharz, D., Ruzicka, T., & Kolb-Bachofen, V. (1998). Nitric oxide and its implications in skin homeostasis and disease – a review. Archives of Dermatological Research, *290*(12), 643-651.

Bystrova, S., & Luttge, R. (2011). Micromolding for ceramic microneedle arrays. Microelectronic Engineering, *88*(8), 1681-1684.

Chadebech, P., Goidin, D., Jacquet, C., Viac, J., Schmitt, D., & Staquet, M.-J. (2003). Use of human reconstructed epidermis to analyze the regulation of β-defensin hBD-1, hBD-2, and hBD-3 expression in response to LPS. Cell Biology and Toxicology, *19*(5), 313-324.

Clarke, G., O'Mahony, S., Malone, G., & Dinan, T. G. (2007). An isocratic high performance liquid chromatography method for the determination of GABA

and glutamate in discrete regions of the rodent brain. Journal of Neuroscience Methods, *160*(2), 223-230.

Cleland, R. L., & Wang, J. L. (1970). Ionic polysaccharides. III. Dilute solution properties of hyaluronic acid fractions. Biopolymers, *9*(7), 799-810.

Corneliu, G. (1968). Use of butyrolactam for treating motion sickness: Google Patents.

Cronin, J. R., Pizzarello, S., & Gandy, W. E. (1979). Amino acid analysis with o-phthalaldehyde detection: effects of reaction temperature and thiol on fluorescence yields. Analytical Biochemistry, *93*, 174-179.

Davis, S. P., Martanto, W., Allen, M. G., & Prausnitz, M. R. (2005). Hollow metal microneedles for insulin delivery to diabetic rats. IEEE Transactions on Biomedical Engineering, *52*(5), 909-915.

Dawson, L. A., Organ, A. J., Winter, P., Lacroix, L. P., Shilliam, C. S., Heidbreder, C., & Shah, A. J. (2004). Rapid high-throughput assay for the measurement of amino acids from microdialysates and brain tissue using monolithic C18-bonded reversed-phase columns. Journal of Chromatography B, *807*(2), 235-241.

de Freitas Silva, D. M., Ferraz, V. P., & Ribeiro, Â. M. (2009). Improved high-performance liquid chromatographic method for GABA and glutamate determination in regions of the rodent brain. Journal of Neuroscience Methods, *177*(2), 289-293.

Denda, M., Inoue, K., Inomata, S., & Denda, S. (2002). γ-aminobutyric acid (A) receptor agonists accelerate cutaneous barrier recovery and prevent epidermal hyperplasia induced by barrier disruption. Journal of Investigative Dermatology, *119*(5), 1041-1047.

Devall, A. J., Blake, R., Langman, N., Smith, C. G. S., Richards, D. A., & Whitehead, K. J. (2007). Monolithic column-based reversed-phase liquid chromatography separation for amino acid assay in microdialysates and cerebral spinal fluid. Journal of Chromatography B, *848*(2), 323-328.

Di Cagno, R., Mazzacane, F., Rizzello, C. G., De Angelis, M., Giuliani, G., Meloni, M., . . . Gobbetti, M. (2010). Synthesis of γ-aminobutyric acid (GABA) by Lactobacillus plantarum DSM19463: functional grape must beverage and dermatological applications. Applied Microbiology and Biotechnology, *86*(2), 731-741.

Diana, M., Quílez, J., & Rafecas, M. (2014). Gamma-aminobutyric acid as a bioactive compound in foods: a review. Journal of Functional Foods, *10*, 407-420.

Donnelly, R. F., Majithiya, R., Singh, T. R. R., Morrow, D. I. J., Garland, M. J., Demir, Y. K., . . . Woolfson, A. D. (2011). Design, optimization and characterisation of polymeric microneedle arrays prepared by a novel laser-based micromoulding technique. Pharmaceutical Research, *28*(1), 41-57.

Donnelly, R. F., Morrow, D. I. J., McCarron, P. A., Woolfson, A. D., Morrissey, A., Juzenas, P., . . . Moan, J. (2008). Microneedle-mediated intradermal delivery of 5-aminolevulinic acid: Potential for enhanced topical photodynamic therapy. Journal of Controlled Release, *129*(3), 154-162.

Donnelly, R. F., Morrow, D. I. J., Singh, T. R. R., Migalska, K., McCarron, P. A., O'Mahony, C., & Woolfson, A. D. (2009). Processing difficulties and

instability of carbohydrate microneedle arrays. Drug Development and Industrial Pharmacy, *35*(10), 1242-1254.

Donnelly, R. F., Singh, T. R. R., Tunney, M. M., Morrow, D. I. J., McCarron, P. A., O'Mahony, C., & Woolfson, A. D. (2009). Microneedle arrays allow lower microbial penetration than hypodermic needles in vitro. Pharmaceutical Research, *26*(11), 2513-2522.

Drain, K. F., Murphy, W. R., & Otterburn, M. S. (1983). Solvents for polypropylene: their selection for a recycling process. Conservation & Recycling, *6*(3), 107-122.

Faler, B. J., Macsata, R. A., Plummer, D., Mishra, L., & Sidawy, A. N. (2006). Transforming growth factor-β and wound healing. Perspectives in Vascular Surgery and Endovascular Therapy, *18*(1), 55-62.

Feldmeyer, L., Werner, S., French, L. E., & Beer, H.-D. (2010). Interleukin-1, inflammasomes and the skin. European Journal of Cell Biology, *89*(9), 638-644.

Gardeniers, H. J. G. E., Luttge, R., Berenschot, E. J. W., Boer, M. J. d., Yeshurun, S. Y., Hefetz, M., . . . Berg, A. v. d. (2003). Silicon micromachined hollow microneedles for transdermal liquid transport. Journal of Microelectromechanical Systems, *12*(6), 855-862.

Gill, H. S., Denson, D. D., Burris, B. A., & Prausnitz, M. R. (2008). Effect of microneedle design on pain in human volunteers. The Clinical Journal of Pain, *24*(7), 585-594.

Gill, H. S., & Prausnitz, M. R. (2007a). Coated microneedles for transdermal delivery. Journal of Controlled Release, *117*(2), 227-237.

Gill, H. S., & Prausnitz, M. R. (2007b). Coating formulations for microneedles. Pharmaceutical Research, *24*(7), 1369-1380.

Godin, B., & Touitou, E. (2007). Transdermal skin delivery: Predictions for humans from in vivo, ex vivo and animal models. Advanced Drug Delivery Reviews, *59*(11), 1152-1161.

Gratieri, T., Alberti, I., Lapteva, M., & Kalia, Y. N. (2013). Next generation intra- and transdermal therapeutic systems: Using non- and minimally-invasive technologies to increase drug delivery into and across the skin. European Journal of Pharmaceutical Sciences, *50*(5), 609-622.

Groves, R. W., Allen, M. H., Ross, E. L., Barker, J. N. W. N., & Macdonald, D. M. (1995). Tumour necrosis factor alpha is pro-inflammatory in normal human skin and modulates cutaneous adhesion molecule expression. British Journal of Dermatology, *132*(3), 345-352.

Gübitz, G., Wintersteiger, R., & Hartinger, A. (1981). Fluorescence derivatization of tertiary amines with 2-naphthyl chloroformate. Journal of Chromatography A, *218*, 51-56.

Han, D., Kim, H.-Y., Lee, H.-J., Shim, I., & Hahm, D.-H. (2007). Wound healing activity of gamma-aminobutyric Acid (GABA) in rats. Journal of Microbiology and Biotechnology, *17*(10), 1661-1669.

Handley, M. K., Hirth, W. W., Phillips, J. G., Ali, S. M., Khan, A., Fadnis, L., & Tedford, C. E. (1998). Development of a sensitive and quantitative analytical method for 1H-4-substituted imidazole histamine H3-receptor antagonists utilizing high-performance liquid chromatography and dabsyl derivatization.

Journal of Chromatography B: Biomedical Sciences and Applications, *716*(1–2), 239-249.

Harder, J., Bartels, J., Christophers, E., & Schroder, J. M. (1997). A peptide antibiotic from human skin. Nature, *387*(6636), 861-861.

Hayakawa, K., Kimura, M., Kasaha, K., Matsumoto, K., Sansawa, H., & Yamori, Y. (2004). Effect of a γ-aminobutyric acid-enriched dairy product on the blood pressure of spontaneously hypertensive and normotensive Wistar–Kyoto rats. British Journal of Nutrition, *92*(3), 411-417.

Hayat, A., Jahangir, T. M., Khuhawar, M. Y., Alamgir, M., Hussain, Z., Haq, F. U., & Musharraf, S. G. (2015). HPLC determination of gamma amino butyric acid (GABA) and some biogenic amines (BAs) in controlled, germinated, and fermented brown rice by pre-column derivatization. Journal of Cereal Science, *64*, 56-62.

Henry, S., McAllister, D. V., Allen, M. G., & Prausnitz, M. R. (1998). Microfabricated microneedles: a novel approach to transdermal drug delivery. Journal of Pharmaceutical Sciences, *87*(8), 922-925.

Hiraishi, Y., Nakagawa, T., Quan, Y.-S., Kamiyama, F., Hirobe, S., Okada, N., & Nakagawa, S. (2013). Performance and characteristics evaluation of a sodium hyaluronate-based microneedle patch for a transcutaneous drug delivery system. International Journal of Pharmaceutics, *441*(1–2), 570-579.

Hirobe, S., Azukizawa, H., Matsuo, K., Zhai, Y., Quan, Y.-S., Kamiyama, F., . . . Nakagawa, S. (2013). Development and clinical study of a self-dissolving microneedle patch for transcutaneous immunization device. Pharmaceutical Research, *30*(10), 2664-2674.

Hsieh, C.-Y., Tsai, E.-M., & Wu, H.-L. (2006). Simple and sensitive liquid chromatographic method with fluorimetric detection for the analysis of γ-amino-n-butyric acid in human urine. Analytica Chimica Acta, *577*(2), 201-206.

ICH, T. I. C. o. H. o. T. R. f. R. o. P. f. H. U. (2005). Validation of analytical procedures: text and methodology. Available from http://www.ich.org/. . Available 1 June 2015 http://www.ich.org/.

Ishikawa, A., Oka, H., Hiemori, M., Yamashita, H., Kimoto, M., Kawasaki, H., & Tsuji, H. (2009). Development of a method for the determination of γ-aminobutyric acid in foodstuffs. Journal of Nutritional Science and Vitaminology, *55*(3), 292-295.

Ito, K., Tanaka, K., Nishibe, Y., Hasegawa, J., & Ueno, H. (2007). GABA-synthesizing enzyme, GAD67, from dermal fibroblasts: Evidence for a new skin function. Biochimica et Biophysica Acta (BBA) - General Subjects, *1770*(2), 291-296.

Iwaki, K., & Kitada, Y. (2007). Availability of partially milled rice as a daily source of gamma-aminobutyric acid. Food Science and Technology Research, *13*(1), 41-44.

Jarry, H., Hirsch, B., Leonhardt, S., & Wuttke, W. (1992). Amino acid neurotransmitter release in the preoptic area of rats during the positive feedback actions of estradiol on LH release. Neuroendocrinology, *56*(2), 133-140.

Jiang, B., Fu, Y., & Zhang, T. (2010). Gamma-aminobutyric acid *Bioactive Proteins and Peptides as Functional Foods and Nutraceuticals* (pp. 121-133): Wiley-Blackwell.

Katagiri, C., Sato, J., Nomura, J., & Denda, M. (2003). Changes in environmental humidity affect the water-holding property of the stratum corneum and its free amino acid content, and the expression of filaggrin in the epidermis of hairless mice. Journal of Dermatological Science, *31*(1), 29-35.

Kaushik, S., Hord, A. H., Denson, D. D., McAllister, D. V., Smitra, S., Allen, M. G., & Prausnitz, M. R. (2001). Lack of pain associated with microfabricated microneedles. Anesthesia and Analgesia, *92*(2), 502-504.

Kenneth, A. W., & Michael, S. R. (2002). The structure and function of skin *Dermatological and Transdermal Formulations* (pp. 1-39): CRC Press.

Kezic, S., Kemperman, P. M. J. H., Koster, E. S., de Jongh, C. M., Thio, H. B., Campbell, L. E., . . . Caspers, P. J. (2008). Loss-of-function mutations in the filaggrin gene lead to reduced level of natural moisturizing factor in the stratum corneum. Journal of Investigative Dermatology, *128*(8), 2117-2119.

Khuhawar, M., & Rajper, A. (2003). Liquid chromatographic determination of γ-aminobutyric acid in cerebrospinal fluid using 2-hydroxynaphthaldehyde as derivatizing reagent. Journal of Chromatography B, *788*(2), 413-418.

Khuhawar, M. Y., & Rajper, A. D. (2003). Liquid chromatographic determination of γ-aminobutyric acid in cerebrospinal fluid using 2-hydroxynaphthaldehyde as derivatizing reagent. Journal of Chromatography B, *788*(2), 413-418.

Kim, M., Yang, H., Kim, H., Jung, H., & Jung, H. (2014). Novel cosmetic patches for wrinkle improvement: retinyl retinoate- and ascorbic acid-loaded dissolving microneedles. International Journal of Cosmetic Science, *36*(3), 207-212.

Kochhar, J. S., Quek, T. C., Soon, W. J., Choi, J., Zou, S., & Kang, L. (2013). Effect of microneedle geometry and supporting substrate on microneedle array penetration into skin. Journal of Pharmaceutical Sciences, *102*(11), 4100-4108.

Kolli, C. S., & Banga, A. K. (2008). Characterization of solid maltose microneedles and their use for transdermal delivery. Pharmaceutical Research, *25*(1), 104-113.

Kong, M., Chen, X. G., Kweon, D. K., & Park, H. J. (2011). Investigations on skin permeation of hyaluronic acid based nanoemulsion as transdermal carrier. Carbohydrate Polymers, *86*(2), 837-843.

Kong, X. Q., Zhou, P., & Wu, C. W. (2011). Numerical simulation of microneedles' insertion into skin. Computer Methods in Biomechanics and Biomedical Engineering, *14*(9), 827-835.

Kormeili, T., Yamauchi, P. S., & Lowe, N. J. (2004). Topical photodynamic therapy in clinical dermatology. British Journal of Dermatology, *150*(6), 1061-1069.

Laden, K. (1967). Moisturizing agent in skin. Journal of the Society of Cosmetic Chemists *18*, 360.

Lane, T., & Lachmann, H. J. (2011). The emerging role of interleukin-1β in autoinflammatory diseases. Current Allergy and Asthma Reports, *11*(5), 361-368.

Laurent, T. C. (1987). Biochemistry of hyaluronan. Acta Oto-Laryngologica, *104*(sup442), 7-24.

Lee, J. W., Park, J.-H., & Prausnitz, M. R. (2008). Dissolving microneedles for transdermal drug delivery. Biomaterials, *29*(13), 2113-2124.

Lee, K. S., & Drescher, D. G. (1978). Fluorometric amino-acid analysis with o-phthaldialdehyde (OPA). The International Journal of Biochemistry, *9*(7), 457-467.

Li, H., Low, Y. S. J., Chong, H. P., Zin, M. T., Lee, C.-Y., Li, B., . . . Kang, L. (2015). Microneedle-mediated delivery of copper peptide through skin. Pharmaceutical Research, *32*(8), 2678-2689.

Lin, W., Cormier, M., Samiee, A., Griffin, A., Johnson, B., Teng, C.-L., . . . Daddona, P. E. (2001). Transdermal delivery of antisense oligonucleotides with microprojection patch (macroflux®) technology. Pharmaceutical Research, *18*(12), 1789-1793.

Luangveera, W., Jiruedee, S., Mama, W., Chiaranairungroj, M., Pimpin, A., Palaga, T., & Srituravanich, W. (2015). Fabrication and characterization of novel microneedles made of a polystyrene solution. Journal of the Mechanical Behavior of Biomedical Materials, *50*, 77-81.

Magnus, L., & Bo, F. (2005). The skin as a barrier *Dry Skin and Moisturizers* (pp. 9-21): CRC Press.

Mañes, J., Gimeno, M. J., Moltó, J. C., & Font, G. (1988). Invited plenary, keynote and submitted papers from the international symposium on pharmaceutical and biomedical analysis fluorimetric determination of hydrazine in isoniazid formulations with 2-hydroxy-1-naphthaldehyde. Journal of Pharmaceutical and Biomedical Analysis, *6*(6), 1023-1027.

Martanto, W., Davis, S. P., Holiday, N. R., Wang, J., Gill, H. S., & Prausnitz, M. R. (2004). Transdermal delivery of insulin using microneedles in vivo. Pharmaceutical Research, *21*(6), 947-952.

Martanto, W., Moore, J. S., Kashlan, O., Kamath, R., Wang, P. M., O'Neal, J. M., & Prausnitz, M. R. (2006). Microinfusion using hollow microneedles. Pharmaceutical Research, *23*(1), 104-113.

Martin, C. J., Allender, C. J., Brain, K. R., Morrissey, A., & Birchall, J. C. (2012). Low temperature fabrication of biodegradable sugar glass microneedles for transdermal drug delivery applications. Journal of Controlled Release, *158*(1), 93-101.

MatWeb, L. (n.d.). Typical compressive yield strength and compressive modulus of polymers. Available from http://www.matweb.com/reference/compressivestrength.aspx Available 5 January 2016 http://www.matweb.com/reference/compressivestrength.aspx

McGrath, J. A., & Uitto, J. (2010). Anatomy and organization of human skin *Rook's Textbook of Dermatology* (pp. 1-53): Wiley-Blackwell.

McKeen, L. W. (2014). 3 - plastics used in medical devices In S. Ebnesajjad (Ed.), *Handbook of Polymer Applications in Medicine and Medical Devices* (pp. 21-53). Oxford: William Andrew Publishing.

Mikolajewska, P., Donnelly, R. F., Garland, M. J., Morrow, D. I. J., Singh, T. R. R., Iani, V., . . . Juzeniene, A. (2010). Microneedle pre-treatment of human skin improves 5-aminolevulininc acid (ALA)- and 5-aminolevulinic acid methyl ester (MAL)-induced PpIX production for topical photodynamic therapy

without increase in pain or erythema. Pharmaceutical Research, *27*(10), 2213-2220.

Mody, I., De Koninck, Y., Otis, T. S., & Soltesz, I. (1994). Bridging the cleft at GABA synapses in the brain. Trends in Neurosciences, *17*(12), 517-525.

Mohammed El-Brashy, A., & Mohammed Al-Ghannam, S. (1997). High-performance liquid chromatographic determination of some amino acids after derivatization with 2-hydroxy-1-naphthaldehyde. Analyst, *122*(2), 147-150.

Mohammed, Y. H., Yamada, M., Lin, L. L., Grice, J. E., Roberts, M. S., Raphael, A. P., . . . Prow, T. W. (2014). Microneedle enhanced delivery of cosmeceutically relevant peptides in human skin. PLoS ONE, *9*(7), e101956.

Molnár-Perl, I. (2001). Derivatization and chromatographic behavior of the o-phthaldialdehyde amino acid derivatives obtained with various SH-group-containing additives. Journal of Chromatography A, *913*(1–2), 283-302.

Nanney, L. B. (1990). Epidermal and dermal effects of epidermal growth factor during wound repair. Journal of Investigative Dermatology, *94*(5), 624-629.

Olatunji, O., Das, D. B., Garland, M. J., Belaid, L., & Donnelly, R. F. (2013). Influence of array interspacing on the force required for successful microneedle skin penetration: theoretical and practical approaches. Journal of Pharmaceutical Sciences, *102*(4), 1209-1221.

Park, J.-H., Allen, M. G., & Prausnitz, M. R. (2005). Biodegradable polymer microneedles: fabrication, mechanics and transdermal drug delivery. Journal of Controlled Release, *104*(1), 51-66.

Park, J.-H., & Prausnitz, M. R. (2010). Analysis of mechanical failure of polymer microneedles by axial force. The Journal of the Korean Physical Society, *56*(4), 1223-1227.

Pavicic, T., Gauglitz, G. G., Lersch, P., Schwach-Abdellaoui, K., Malle, B., Korting, H. C., & Farwick, M. (2011). Efficacy of cream-based novel formulations of hyaluronic acid of different molecular weights in anti-wrinkle treatment. Journal of Drugs in Dermatology : JDD, *10*(9), 990-1000.

Pierce, G. F., Mustoe, T. A., Lingelbach, J., Masakowski, V. R., Griffin, G. L., Senior, R. M., & Deuel, T. F. (1989). Platelet-derived growth factor and transforming growth factor-beta enhance tissue repair activities by unique mechanisms. The Journal of Cell Biology, *109*(1), 429-440.

Pierce, G. F., Tarpley, J. E., Yanagihara, D., Mustoe, T. A., Fox, G. M., & Thomason, A. (1992). Platelet-derived growth factor (BB homodimer), transforming growth factor-beta 1, and basic fibroblast growth factor in dermal wound healing. Neovessel and matrix formation and cessation of repair. The American Journal of Pathology, *140*(6), 1375-1388.

Puneet, K., Kevin, L., Joel, A. S., & Shekhar, B. (2010). Sharpening of hollow silicon microneedles to reduce skin penetration force. Journal of Micromechanics and Microengineering, *20*(4), 045011.

Roberts, E., & Frankel, S. (1950). γ-aminobutyric acid in brain: its formation from glutamic acid. Journal of Biological Chemistry, *187*, 55-63.

Römgens, A. M., Bader, D. L., Bouwstra, J. A., Baaijens, F. P. T., & Oomens, C. W. J. (2014). Monitoring the penetration process of single microneedles with varying tip diameters. Journal of the Mechanical Behavior of Biomedical Materials, *40*, 397-405.

Sastri, V. R. (2014). 3 - materials used in medical devices *Plastics in Medical Devices (Second Edition)* (pp. 19-31). Oxford: William Andrew Publishing.

Sayo, T., Sugiyama, Y., Takahashi, Y., Ozawa, N., Sakai, S., Inoue, S., . . . Tamura, M. (2002). Hyaluronan synthase 3 regulates hyaluronan synthesis in cultured human keratinocytes. Journal of Investigative Dermatology, *118*(1), 43-48.

Schröder, J.-M., & Harder, J. (1999). Human beta-defensin-2. The International Journal of Biochemistry & Cell Biology, *31*(6), 645-651.

Scott, J. E., Cummings, C., Brass, A., & Chen, Y. (1991). Secondary and tertiary structures of hyaluronan in aqueous solution, investigated by rotary shadowing-electron microscopy and computer simulation. Hyaluronan is a very efficient network-forming polymer. Biochemical Journal, *274*(3), 699-705.

Scutt, A., Meghji, S., & Harvey, W. (1987). Stimulation of human fibroblast collagen synthesis in vitro by γ-aminobutyric acid. Biochemical Pharmacology, *36*(8), 1333-1335.

Shah, A. J., Crespi, F., & Heidbreder, C. (2002). Amino acid neurotransmitters: separation approaches and diagnostic value. Journal of Chromatography B, *781*(1–2), 151-163.

Sheng, W., Hang, H.-W., & Ruan, D.-Y. (2005). In vivo microdialysis study of the relationship between lead-induced impairment of learning and neurotransmitter changes in the hippocampus. Environmental Toxicology and Pharmacology, *20*(1), 233-240.

Sirsjö, A., Karlsson, M., GidöF, A., Rollman, O., & TÖRmÄ, H. (1996). Increased expression of inducible nitric oxide synthase in psoriatic skin and cytokine-stimulated cultured keratinocytes. British Journal of Dermatology, *134*(4), 643-648.

Sobotka, L., Smahelova, A., Pastorova, J., & Kusalova, M. (2007). A case report of the treatment of diabetic foot ulcers using a sodium hyaluronate and iodine complex. The International Journal of Lower Extremity Wounds, *6*(3), 143-147.

Soghomonian, J.-J., & Martin, D. L. (1998). Two isoforms of glutamate decarboxylase: why? Trends in Pharmacological Sciences, *19*(12), 500-505.

Sugiyama, Y., Shimada, A., Sayo, T., Sakai, S., & Inoue, S. (1998). Putative hyaluronan synthase mRNA are expressed in mouse skin and TGF-β upregulates their expression in cultured human skin cells. Journal of Investigative Dermatology, *110*(2), 116-121.

Sunol, C., Artigas, F., Tusell, J. M., & Gelpi, E. (1988). High-performance liquid chromatography-fluorescence detection method for endogenous γ-aminobutyric acid validated by mass spectrometric and gas chromatographic techniques. Analytical Chemistry, *60*(7), 649-651.

Takahashi, H., Sumi, M., & Koshino, F. (1961). Effect of γ-aminobutyric acid (GABA) on normotensive or hypertensive rats and men. The Japanese Journal of Physiology, *11*(1), 89-95.

Torezan, L., Chaves, Y., Niwa, A., Sanches, J. A., Festa-Neto, C., & Szeimies, R.-M. (2013). A pilot split-face study comparing conventional methyl aminolevulinate-photodynamic therapy (PDT) with microneedling-assisted PDT on actinically damaged skin. Dermatologic Surgery, *39*(8), 1197-1201.

Tracey, K. J., & Cerami, A. (1994). Tumor necrosis factor: a pleiotropic cytokine and therapuetic target. Annual Review of Medicine, *45*(1), 491-503.

van der Maaden, K., Jiskoot, W., & Bouwstra, J. (2012). Microneedle technologies for (trans)dermal drug and vaccine delivery. Journal of Controlled Release, *161*(2), 645-655.

van der Maaden, K., Trietsch, S. J., Kraan, H., Varypataki, E. M., Romeijn, S., Zwier, R., . . . Bouwstra, J. (2014). Novel Hollow Microneedle Technology for Depth-Controlled Microinjection-Mediated Dermal Vaccination: A Study with Polio Vaccine in Rats. Pharmaceutical Research, *31*(7), 1846-1854.

Varanyanond, W., Tungtrakul, P., Surojanametakul, V., Watanasiritham, L., & Luxiang, W. (2005). Effect of water soaking on gamma-aminobutyric acid (GABA) in germ of different Thai rice varieties. Kasetsart Journal (Natural Science) *39*, 411-415.

Verbaan, F. J., Bal, S. M., van den Berg, D. J., Dijksman, J. A., van Hecke, M., Verpoorten, H., . . . Bouwstra, J. A. (2008). Improved piercing of microneedle arrays in dermatomed human skin by an impact insertion method. Journal of Controlled Release, *128*(1), 80-88.

Verbaan, F. J., Bal, S. M., van den Berg, D. J., Groenink, W. H. H., Verpoorten, H., Lüttge, R., & Bouwstra, J. A. (2007). Assembled microneedle arrays enhance the transport of compounds varying over a large range of molecular weight across human dermatomed skin. Journal of Controlled Release, *117*(2), 238-245.

Wang, P. M., Cornwell, M., Hill, J., & Prausnitz, M. R. (2006). Precise microinjection into skin using hollow microneedles. Journal of Investigative Dermatology, *126*(5), 1080-1087.

Wolf, J. E., Taylor, J. R., Tschen, E., & Kang, S. (2001). Topical 3.0% diclofenac in 2.5% hyaluronan gel in the treatment of actinic keratoses. International Journal of Dermatology, *40*(11), 709-713.

Yan, G., Warner, K. S., Zhang, J., Sharma, S., & Gale, B. K. (2010). Evaluation needle length and density of microneedle arrays in the pretreatment of skin for transdermal drug delivery. International Journal of Pharmaceutics, *391*(1–2), 7-12.

Yunger, L. M., & Cramer, R. D. (1981). Measurement and correlation of partition coefficients of polar amino acids. Molecular Pharmacology, *20*(3), 602-608.

Appendix

Raw data

Table 13 Needle widths at three measuring points: 0.5, 1 and 1.5 mm from the tip (before selection)

Order	Reference point at 0.5 mm	Reference point at 1.0 mm	Reference point at 1.5 mm
1	105.48	140.95	171.00
2	101.37	139.30	171.00
3	102.28	144.54	179.58
4	103.72	134.07	160.70
5	105.87	138.00	168.13
6	96.15	143.05	182.01
7	106.98	145.42	178.91
8	108.50	140.47	166.39
9	107.94	146.66	176.71
10	97.55	136.75	167.00
11	103.33	144.28	176.48
12	96.44	130.80	159.10
13	95.15	127.76	159.40
14	101.75	143.93	179.26
15	108.54	139.11	167.56
16	114.65	143.10	160.43
17	110.04	142.69	168.82
18	96.45	133.12	162.76
19	101.94	144.99	178.81
20	103.43	148.24	180.07
21	106.86	142.22	171.42
22	127.91	154.47	177.43
23	119.68	156.17	185.26
24	103.86	135.22	164.80
25	95.62	136.23	167.46
26	95.25	138.18	167.46
27	111.88	150.55	178.21
28	100.49	137.40	171.07
29	104.68	146.57	181.90
30	101.64	146.18	176.84
31	103.38	147.31	179.01
32	106.81	151.31	184.83

33	106.15	151.24	183.08
34	101.69	141.07	175.30
35	85.56	130.66	164.07
36	96.88	143.54	172.10
37	106.23	152.07	183.57
38	93.65	138.70	173.58
39	108.91	140.81	165.74
40	118.17	147.15	171.80
41	115.46	145.07	170.13
42	120.90	150.13	174.97
43	116.70	148.06	171.11
44	120.44	149.23	170.46
45	108.59	138.65	161.96
46	117.41	147.60	171.84
47	122.82	154.44	173.54
48	125.22	153.74	173.82
49	127.22	154.78	180.03
50	123.31	154.92	174.83
51	116.09	148.60	170.41
52	130.50	158.06	176.10
53	111.46	141.70	164.78
54	115.69	153.24	175.72
55	117.01	150.14	172.27
56	117.66	147.84	170.90
57	117.66	146.33	166.92
58	119.38	149.56	169.32
59	119.10	149.82	169.04
60	122.74	153.59	170.30
61	124.74	157.94	176.89
62	115.80	145.03	168.85
63	116.64	145.54	166.41
64	124.26	150.60	172.19
65	117.58	147.29	170.89
66	124.79	152.85	170.89
67	116.79	148.56	170.69
68	120.58	150.88	175.58
69	101.73	145.62	179.89
70	99.01	141.48	170.51
71	109.16	149.25	173.75
72	100.48	149.58	180.08
73	100.48	141.62	170.20

74	102.57	147.43	182.06
75	99.64	142.83	175.76
76	105.66	142.69	171.77
77	101.15	141.93	171.16
78	94.83	145.15	178.22
79	101.77	140.61	165.10
80	101.71	145.55	173.52
81	99.88	145.06	176.99
82	99.86	145.79	178.36
83	96.74	132.02	160.28
84	105.32	147.75	178.19
85	83.87	131.44	165.10
86	107.15	146.11	180.14
87	104.21	144.83	172.78
88	100.36	146.70	179.27
89	102.93	136.24	163.56
90	94.09	145.76	181.83
91	87.41	132.96	169.34
92	119.80	155.87	181.96
93	103.57	143.97	179.62
94	104.78	147.05	178.12
95	99.84	139.67	167.72
96	112.05	143.35	175.62
97	101.70	144.70	175.50
98	107.26	144.11	171.42
99	102.94	143.49	173.22
100	90.43	132.12	162.15
101	101.25	146.75	179.10
102	103.08	145.80	180.02
103	94.79	140.32	174.23
104	95.59	139.50	171.11
105	102.72	142.55	177.87
106	105.13	146.30	179.00
107	109.52	143.11	172.31
108	109.30	146.53	171.44
109	121.42	165.05	190.15
110	95.00	138.29	168.32
111	98.41	139.20	173.61
112	109.42	139.06	162.68
113	115.94	145.37	168.46
114	129.53	154.36	171.93

115	119.65	149.29	169.20
116	105.12	141.24	165.46
117	121.55	150.80	174.92
118	118.34	144.32	170.49
119	118.34	151.54	175.25
120	122.88	155.77	174.52
121	118.27	147.01	168.17
122	92.92	132.73	160.39
123	116.92	150.32	170.23
124	111.21	144.21	167.07
125	122.31	151.40	176.99
AVG	**108.08**	**144.97**	**172.69**
SD	**10.16**	**6.51**	**6.18**

Table 14 Needle widths at three measuring points: 0.5, 1 and 1.5 mm from the tip (after selection)

Order	Reference point at 500 micron	Reference point at 1000 micron	Reference point at 1500 micron
1	105.48	140.95	171.00
2	101.37	139.30	171.00
3	102.28	144.54	179.58
4	105.87	138.00	168.13
5	106.98	145.42	178.91
6	108.50	140.47	166.39
7	107.94	146.66	176.71
8	103.33	144.28	176.48
9	101.75	143.93	179.26
10	108.54	139.11	167.56
11	114.65	143.10	160.43
12	110.04	142.69	168.82
13	101.94	144.99	178.81
14	103.43	148.24	180.07
15	106.86	142.22	171.42
16	111.88	150.55	178.21
17	100.49	137.40	171.07
18	104.68	146.57	181.90
19	101.64	146.18	176.84
20	103.38	147.31	179.01
21	106.81	151.31	184.83
22	106.15	151.24	183.08
23	101.69	141.07	175.30
24	96.88	143.54	172.10
25	93.65	138.70	173.58
26	108.91	140.81	165.74
27	118.17	147.15	171.80
28	115.46	145.07	170.13
29	120.90	150.13	174.97
30	116.70	148.06	171.11
31	120.44	149.23	170.46
32	108.59	138.65	161.96

33	117.41	147.60	171.84
34	116.09	148.60	170.41
35	111.46	141.70	164.78
36	115.69	153.24	175.72
37	117.01	150.14	172.27
38	117.66	147.84	170.90
39	117.66	146.33	166.92
40	119.38	149.56	169.32
41	119.10	149.82	169.04
42	115.80	145.03	168.85
AVG	**109.35**	**145.16**	**172.78**
SD	**7.01**	**4.12**	**5.53**

Table 15 Displacement against force (N)/needle of 1 mm dipping size MNs

Scale (mm)	Force (N)/Needle Piece no.1	Force (N)/Needle Piece no.2	Force (N)/Needle Piece no.3	Force (N)/Needle Piece no.4	Force (N)/Needle Piece no.5	Force (N)/Needle Piece no.6	Mean	SD
0.0000	0.0000	0.0000	0.0000	0.0000	0.0000	0.0000	0.0000	0.0000
0.0508	0.0047	0.0029	0.0191	0.0208	0.0652	0.0037	0.0194	0.0217
0.1016	0.1740	0.0176	0.0066	0.0760	0.1825	0.0267	0.0806	0.0724
0.1524	0.3063	0.1000	0.1786	0.1727	0.3050	0.1316	0.1990	0.0798
0.2032	0.4256	0.2323	0.2690	0.3148	0.4344	0.2359	0.3187	0.0833
0.2540	0.5733	0.3719	0.3891	0.4295	0.5544	0.3724	0.4484	0.0840
0.3048	0.7105	0.4944	0.5143	0.5709	0.7063	0.4998	0.5827	0.0923
0.3556	0.8580	0.6635	0.6368	0.7313	0.8411	0.6395	0.7283	0.0913
0.4064	1.0123	0.8154	0.7700	0.9298	1.0273	0.7786	0.8889	0.1063
0.4572	1.1777	0.9771	0.9214	1.1356	1.2600	0.9281	1.0666	0.1309
0.5080	1.4460	1.1510	1.0836	1.3855	1.4916	1.1559	1.2856	0.1601
0.5588	1.6885	1.4034	1.3054	1.6207	1.7211	1.3899	1.5215	0.1610
0.6096	1.9274	1.6239	1.5357	1.8289	1.9590	1.6709	1.7576	0.1577
0.6604	2.1614	1.8419	1.8738	2.1474	2.2866	1.9448	2.0426	0.1648
0.7112	2.4076	1.9350	2.1482	2.3998	2.5811	2.2780	2.2916	0.2069
0.7620	2.6428	2.2658	2.4397	2.6913	2.7729	2.5948	2.5679	0.1690
0.8128	2.9344	2.5524	2.6578	2.9461	2.9750	2.9040	2.8283	0.1621
0.8636	3.2333	2.8905	3.0130	3.1985	3.2176	3.1948	3.1246	0.1279
0.9144	3.4832	3.1845	3.3119	3.4484	3.5067	3.6304	3.4275	0.1434
0.9652	3.8213	3.4785	3.6255	3.6248	3.7027	3.8583	3.6852	0.1283
1.0160	4.1251	3.7652	3.9195	3.8183	4.0016	4.1768	3.9677	0.1502
1.0668	4.3603	3.9930	4.2503	4.0805	4.3666	4.4781	4.2548	0.1695
1.1176	4.7057	4.2870	4.5565	4.2691	4.5430	4.7329	4.5157	0.1820
1.1684	5.0340	4.6251	4.9804	4.4798	4.7954	5.0318	4.8244	0.2124
1.2192	5.4138	4.9730	5.3136	4.7273	5.0281	5.3405	5.1327	0.2435
1.2700	5.7151	5.1470	5.7031	4.9919	5.2952	5.5904	5.4071	0.2795
1.3208	6.0042	5.4189	5.9604	5.2148	5.4177	5.7276	5.6239	0.2945
1.3716	6.2982	5.7815	6.3940	5.5505	5.7019	6.1833	5.9849	0.3202

Table 16 Displacement against force (N)/needle of 1.5 mm dipping size MNs

Scale (mm)	Force (N)/Needle Piece no.1	Force (N)/Needle Piece no.2	Force (N)/Needle Piece no.3	Force (N)/Needle Piece no.4	Force (N)/Needle Piece no.5	Force (N)/Needle Piece no.6	Mean	SD
0.0000	0.0000	0.0000	0.0000	0.0000	0.0000	0.0000	0.0000	0.0000
0.0508	0.0103	0.1134	0.0147	0.1024	0.0179	0.0174	0.0460	0.0440
0.1016	0.2467	0.1975	0.1046	0.1624	0.0987	0.0701	0.1467	0.0616
0.1524	0.3859	0.3236	0.2401	0.2604	0.2176	0.1656	0.2655	0.0717
0.2032	0.5245	0.4694	0.4023	0.3594	0.3491	0.2849	0.3983	0.0794
0.2540	0.6493	0.5961	0.5672	0.4902	0.4846	0.4079	0.5325	0.0801
0.3048	0.8058	0.7578	0.7250	0.6306	0.6257	0.5346	0.6799	0.0917
0.3556	0.9871	0.9043	0.8992	0.7776	0.7642	0.6600	0.8321	0.1087
0.4064	1.2689	1.0905	1.1503	0.9259	0.9195	0.7637	1.0198	0.1676
0.4572	1.4992	1.3379	1.3977	1.0937	1.0486	1.1348	1.2520	0.1683
0.5080	1.7907	1.6111	1.6378	1.3950	1.0689	1.3431	1.4745	0.2357
0.5588	2.0607	1.8662	1.9245	1.6670	1.2196	1.5415	1.7132	0.2781
0.6096	2.3150	2.1215	2.1621	1.9438	1.3666	1.8208	1.9550	0.3067
0.6604	2.6409	2.4441	2.5149	2.3040	1.6141	2.0683	2.2644	0.3415
0.7112	2.9515	2.7455	2.7893	2.6102	1.8052	2.2949	2.5328	0.3826
0.7620	3.2534	3.0297	3.0441	2.8957	2.0061	2.6073	2.8060	0.4071
0.8128	3.5523	3.3580	3.3038	3.2252	2.1751	2.8033	3.0696	0.4594
0.8636	3.8340	3.6275	3.5978	3.5265	2.3589	3.0556	3.3334	0.4952
0.9144	4.1256	3.9117	3.8967	3.8009	2.6039	3.4182	3.6262	0.5038
0.9652	4.3828	4.2057	4.2642	4.0998	2.8881	3.6485	3.9149	0.5140
1.0160	4.7381	4.5217	4.5778	4.4208	3.1551	3.9033	4.2195	0.5419
1.0668	5.0811	4.8280	4.8890	4.7025	3.4246	4.1630	4.5147	0.5637
1.1176	5.3922	5.1073	5.1830	4.9720	3.6451	4.4448	4.7907	0.5889
1.1684	5.7328	5.4307	5.4917	5.2856	3.8828	4.7461	5.0949	0.6197
1.2192	6.0170	5.6830	5.6485	5.5625	4.1376	5.0083	5.3428	0.6160
1.2700	6.2963	5.9721	5.9719	5.8957	4.4193	5.4517	5.6678	0.6107
1.3208	6.6883	6.3127	6.4937	6.1529	4.8138	5.7898	6.0419	0.6164
1.3716	7.1023	6.6802	6.9837	6.5253	5.1666	6.1573	6.4359	0.6456

VITA

Mr. Kritchapol Panrod was born on March 26, 1991 in Bangkok, Thailand. His bachelor's degree was obtained from the Faculty of Science, Kasetsart University with a major in Biochemistry department (second class honors) in 2012. After that, he started this Master's degree program in 2012 at Chulalongkorn University.